Manuscript (non-LaTeX)
Click here to download Manuscript (non-LaTeX) tide_R1_Final.pdf

Analysis of tidal amplitude changes using the EMD method

Yongcun Cheng[1*], Tal Ezer[1], Larry P. Atkinson[1], Hans-Peter Plag[2], Qing Xu[3]

[1]Center for Coastal Physical Oceanography, Old Dominion University, Norfolk, VA, USA

[2]Mitigation and Adaptation Research Institute, Old Dominion University, Norfolk, VA, USA

[3]College of Oceanography, Hohai University, Nanjing, Jiangsu, China

* Corresponding author: y1cheng@odu.edu

Abstract:

Empirical Mode Decomposition/Hilbert-Huang transformation (EMD/HHT) has been used for various geophysical data, including analysis of sea level records to detect trends in sea level rise (SLR) and decadal variations. However, application of EMD to high-frequency sea level variability is less common, so it is tested here as a tool to analyze hourly sea level data and to detect time-dependent changes in tidal amplitudes. The advantage of the EMD over a standard Harmonic Analysis (HA) is that it can detect changes in tidal properties over time with one calculation of an entire record, while HA will require multiple calculations over shorter subsection records; here the two methods are compared. The highest and second-highest frequency modes of the EMD represent the semi-diurnal and diurnal tides, respectively, with especially high correlation between the variations of EMD first mode and M_2 tidal amplitude obtained from HA. High agreements are obtained between HA and EMD mode 1 derived M_2 amplitude and validated by an independent regional tidal solution. The modulation of nodal cycle estimated from EMD mode 1 is about 2-3% of M_2 tide amplitude. Moreover, the amplitude of the M_2 tide seems to slowly increase over time in most stations along the U.S. East Coast (probably due to SLR), but at some locations, such as Wilmington, NC, a much larger increase in the M_2 tide is likely due to local morphological changes associated with sediment movements and erosion. The analysis also shows some interannual variations in tidal amplitudes at some locations that may relate to local man-made changes such as dredging or shoreline structures.

Keywords: tide, EMD, harmonic analysis, sea level

1. Introduction

The U.S. Northeastern coast has been seen as a 'hotspot' of with acceleration in sea level rise (SLR, Sallenger et al., 2012; Ezer and Corlett, 2012) and flooding (Ezer and Atkinson, 2014). The region shows significantly higher trend than global mean SLR (Church and White, 2011; Houston and Dean, 2011). This is due to a combination of land subsidence and potential slowdown of the Atlantic Meridional Overturning Circulation (AMOC) and a weakening of the Gulf Stream (GS) flow (Ezer et al., 2013; Ezer, 2015). SLR increases the damage to low-lying coastal communities during storm surges (Tebaldi et al., 2012; Wahl et al., 2014; Wdowinski et al., 2016) and also increase the frequency of minor tidal flooding (Ezer and Atkinson, 2014; Sweet et al., 2014). Since minor flooding is directly related to the combination of SLR and tidal amplitude, it is important to detect any changes in the characteristics of tides over time.

Recent studies have demonstrated the increases of the M_2 tidal amplitude in the Gulf of Maine (Ray, 2006; 2009) and along the U.S. East Coast (Woodworth, 2010). Coherent linear trends of tidal range in the last 30-90 years have been reported over the regions (Flick et al., 2003). Müller et al. (2011) pointed out that the physical causes of tide trends and their spatial variability are uncertain and it is difficult to relate them to other oceanic or atmospheric variables. Future SLR can affect tides in coastal regions (Pelling et al., 2013). Numerical modeling experiments of the impact of future SLR on tides demonstrate very different local response, so that for the same SLR rate, tidal energy may increase on one coast and decrease in another nearby coasts (Lee et al., 2016). Although the glacial isostatic adjustment and SLR contribute to the trend of M_2 tidal amplitude, the numerical simulations could not reproduce the spatial pattern of the tidal trend (Müller et al, 2011).

At some tide gauge locations, the changes in M_2 tidal amplitude are significant compared with the SLR trend (Müller et al, 2011). This study motivated by the fact that considerable variability of tides may increase the flooding risk when combined with the sea level rise acceleration in the study area (Greenberg et al., 2012; Ezer and Atkinson, 2014), particularly for the low-lying populated regions (e.g., Hampton Roads, south Florida, Miami Beach) vulnerable to SLR (Zhang, 2011; Zhang and Sheng, 2013; Atkinson et al., 2013; Wdowinski et al., 2016).

One of the typical methods used to study the changes in tides is harmonic analysis (HA, (Foreman, 1977) applied to hourly sea level records, though the impact of the sinusoidal nodal cycle (18.61 years) need to be corrected (Müller et al, 2011). In this way, the trends and variability of amplitude and phases of each semi-diurnal and diurnal tide constituents are determined. Note however, that the changes in tidal characteristics due to SLR and other climatic changes can be very different between one region to another (Woodworth, 2010).

In this work, we aim to study the possibility of using Empirical Mode Decomposition (EMD) analysis (Huang et al., 1998, Huang and Wu, 2008) to describe the M_2 tidal amplitude variability by comparing the EMD with that computed using standard HA. The EMD/HHT method is especially useful for non-stationary and nonlinear time series, so that irregular patterns of storm surges, or tidal amplitude changes over time are good test cases for this method. The method decomposes any time series data into a finite number of intrinsic mode functions with time-variable amplitudes and frequencies; the number of modes is determined by the length of the record and the intrinsic variability of the time series. It has been widely used for analysis of many kinds of geophysical data (Wu and Huang, 2009).

Recently, the method has been applied to calculate SLR trends and acceleration and long term sea level variations (e.g., Ezer, 2013; 2015; Bonaduce et al., 2016; Ezer et al., 2016; Cheng et al., 2016). The method was also used to sea level reconstruction (e.g., Sha et al., 2015) and calculate future projections of local SLR based on extrapolation of past SLR rates and acceleration (Ezer and Corlett, 2012). Here it is used to analyze the high-frequency modes to test if they can describe the variability of the M_2 tidal amplitude. Note that because EMD is a non-stationary method, it can detect time-dependent changes in amplitude and frequency with one calculation of an entire record, while the HA will require multiple calculations, each one using a small sub-sections of the data (say 1 year) to calculate how the tides changing over time. On the other hand, the disadvantage of the EMD is that it is a non-parametric method (frequencies are not specified) and thus it cannot guarantee to extract a particular tidal constituent. Therefore, the proposed EMD analysis needs to be tested against standard methods.

The paper is organized as follows. The tide gauge sea level records and the methodology employed in this study are described in section 2. The results are presented in section 3 and the discussion and summary are provided in section 4.

2. Dataset and methodology

a. Tide gauge sea level records

In this study, hourly tide gauge data were downloaded from NOAA (http://opendap.co-ops.nos.noaa.gov/dods/). Figure 1 shows the locations of the selected 17 tide gauges along the U.S. coast. In Table 1, most stations provide long and continuous sea level records (average starting year ~1917) except 2 stations in the lower Chesapeake Bay starting in the 1970s' (No. 10 and 11). The 2 shorter records are included because they are located in a region with significant land subsidence (Kopp, 2013). Our study includes more stations that in a previous study of the issue (Müller, 2011).

b. Harmonic Analysis

The standard tool for tidal analysis is usually based on HA; available software includes for example, TASK (Tidal Analysis Software Kit, (Bell et al., 1996), T-tide (Pawlowicz et al., 2002) and Utide (Codiga, 2011). The Utide was selected to calculate all tidal constituents for its capability in solving the nodal cycle with the default settings. The HA is applied to data sections over two adjacent calendar years (this reduces the effect of data gaps compared with a single year analysis). Therefore, for a record over 1911-2016 for example, the HA is performed for the periods 1911-1912, 1912-1913, …, 2014-2015, 2015-2016. Experiments (not shown) with averaging windows of 1, 2 or 3 years show very little effect on the results. Then the derived variations of the M_2 tidal amplitude (with estimated errors on 95% confidence level) could be used to compare with that computed from EMD method.

c. Empirical Mode Decomposition

To use EMD/HHT to detect changes in tidal amplitudes, we analyze the high frequency modes obtained for each station. An EMD of a sea level record from location M (or from regional mean) would be represented by

$$h^M(\mathrm{t}) = \sum_{i=1}^{N} c_i^M(\mathrm{t}) + r^M(\mathrm{t}) \qquad (1)$$

where N denotes a finite number, $c_i(t)$ is intrinsic oscillatory modes, and $r(t)$ is a residual “trend”. Particular time dependent modes not necessarily represent specific processes, but the analysis allows to evaluate relations between different data that may depend on different time scales. Statistical confidence levels for EMD modes can be calculated using either a bootstrap method (Ezer and Corlett, 2012) or ensemble simulations (Ezer et al., 2016). However, no quantitative examination of each mode is done here, only the 2-year average magnitude of the peaks of the highest frequency EMD mode is examined, to test if it is consistent with changed in the amplitude of M_2 obtained by the HA. Appendix Figure A1 shows an example of the 19 EMD modes for station Baltimore.

In order to keep the consistency between the EMD analysis and HA, we adopt the least-square fitting method in Müller (2011) to remove the linear trend and the nodal cycle in EMD first mode and HA results, i.e.,

$$A_{M_2}(t) = A_0 + At + A_N \sin\left(\frac{2\pi}{18.5996}(t - 1973.66)\right) + A_N \cos\left(\frac{2\pi}{18.5996}(t - 1973.66)\right) \quad (2)$$

The trend term *A* and the cosine/sine nodal terms are removed (Woodworth, 2011; Mawdsley et al., 2015), to reduce the effects of nodal cycle on M_2 tidal amplitude variations.

3. Results

Previous studies show that the tide gauge stations in the study area have mostly positive trend in M_2 amplitude and negative trend at Newport (Müller et al., 2011), and the results presented below are generally consistent with that study. Negative amplitude changes at Chesapeake Bay Bridge Tunnel, Lewes and Sewells Point (Norfolk) are also shown in Woodworth (2010). The largest and most interesting trend occurs at Wilmington, where the tide gauge location upriver is strongly affected by sediment accumulation, as previously indicated (Ray, 2009; Ezer and Atkinson, 2014).

Figure 2a shows the hourly sea level time series (m) estimated with EMD analysis (the first mode, in blue). The black curve presents the M_2 amplitude estimated using HA (section 2b) at Wilmington. The red curve denotes sea level variation magnitude of the EMD first mode, which computed from the peaks of EMD first mode (section 2c). The difference in tidal amplitude variation between the two methods is quite small (~5%) and mainly associated with the 18.6 nodal cycle (Figure 2c), which is absent from the HA analysis (where only M_2 frequency is extracted), but still impact the EMD analysis if not explicitly removed.

Figures 2d-2f are similar to Figures 2a-2c but at Eastport (Gulf of Maine), where the mean M_2 amplitude reaches up to 2.6 m. The significant differences between the sea level time series are also dominated by nodal cycle (Figure 2f), as explain before. Table 1 shows the mean values of M_2 tidal amplitude and EMD analyzed sea level magnitude (mode 1) at all sites after the nodal cycle removed. The M_2 tidal amplitude varies from ∼0.2 m (Baltimore, Key West, No 2 and 10 in Figure 1) to ∼2.6 m (Eastport, No 8 in Figure 1). The mean values of EMD first mode are coherent with that calculated from HA (Table 1).

The period of EMD mode 1 is shown in Figures 2b and 2d for tide gauge Wilmington and Eastport (see Appendix Figure A2 for mode 2), respectively. At Wilmington/Eastport, the mean periods of 12.97/13.01 and 24.34/24.23 hours of the first 2 modes are consistent with periods of the semidiurnal and diurnal tide, respectively. The nodal cycle contributes to the differences between the high frequency mean periods and semidiurnal/diurnal tides in all stations. Table 1 summarizes the mean periods of the EMD high frequency modes at all sites. The calculated mean periods of EMD mode 1 and 2 are consistent with the periods of semi-diurnal and diurnal tides at most of tide gauges, respectively (see discussion below on the more peculiar results at Newport).

Comparison between Fig. 2d with Fig. 2f also suggests a significant M_2 time amplitude trend exists at Wilmington, which has been found in earlier studies (e.g., Müller, 2011). On the other hand, it also implies the modulation of nodal cycle may different at the sites. The EMD method could not provide the sea level variations at a given frequency. We estimate the modulation of nodal cycle to M_2 tide amplitude in EMD mode 1 with Eq. (2). The results are overlaid in Fig. 2c and 2f for Wilmington and Eastport, respectively. The nodal cycle modulations of 0.7 cm and 6.0 cm are refered to the M_2 tide amplitudes of 0.61 m and 2.75 m at the two sites. The modulations of nodal cycle are also listed in Table 1. The amplitude of nodal cycle estimated from EMD mode 1 varies from 1 cm to 6 cm at the sites (~ 2-3% of EMD derived mean amplitude in Table 1). Compare with M_2 tide amplitude, the signal is high at Baltimore (9%) and Key west (7%), which may relate to the instrument change at the sites (see discussion below on the more peculiar results at the sites). Note the signal has been removed to calculate the HA and EMD mode 1 mean M_2 tide amplitude (Table 1).

Figure 3 shows the variations of M_2 amplitude estimated from the HA and the EMD methods at all selected stations. The nodal cycle and mean values in Table 1 have been removed at each tide gauge and the correlation coefficients between the time series are listed in the table. The correlations are higher than 0.6 at most of the sites and reach up to ~1.0 at Wilmington (which shows the largest increase in tidal amplitude of any station). Low correlations are presented at Atlantic City and Sewells Point (Norfolk) and the lowest correlation observed at Newport. The Atlantic City station faces the open Atlantic Ocean, so that the magnitude of sea level variations in the EMD first mode maybe affected by coastal or offshore ocean circulation changes. Clear shifts in amplitude and phase of tidal constituents may attributes to small changes in tide gauge location or surrounding coastal morphology (Mawdsley et al., 2015). Both the Newport and Sewells Point locate inside the harbors, and harbor alteration impact the variations of tidal constituents (Jay, 2009). The mean periods of EMD mode 1 and 2 show high discrepancies with the periods of semidiurnal and diurnal tide at Newport. Notes the M_2 amplitude jumps at Baltimore and Key West in 1960-1970 and the EMD show stronger sea level variations than HA, which could be related to changes in the tide gauge instruments, e.g., there was a reported tide gauge instrument exchanges in 1967 at Key West. Significant variations in the calculated period of sea level are shown at that time period, when the mean periods of 11.98 and 20.02 in EMD mode 1 and 2, respectively, were found. At Pulaski, the data gaps in 1974 is also due to the tide gauge instrument change, which captured by the two approaches. At Fernandina, the jump in the M_2 amplitude in 1905 are shown in the two methods, which are not reported in existing publications. Consist with Müller et al. (2011), high temporal M_2 amplitude variability presented with the two methods is coherent in the Gulf of Maine (Eastport, Portland and Boston). Strong variability is also shown in the South Atlantic Bight (Charleston, Fernandina and Pulaski). The stations at the Mid-Atlantic Bight region demonstrate relatively lower temporal M_2 amplitude variability, with the M_2 amplitude decreasing in the Chesapeake Bay (Chesapeake Bay Bridge Tunnel, Kiptopeke and Sewells Point) and in the Delaware Bay (Lewes) from HA. The phase lag of 1 year between EMD and HA analysis is shown at Kiptopeke. The correlation increases from 0.63 to 0.90 when the phase lag is adjusted in the time series.

In order to further evaluate the robustness of the results, an independent OTIS (Oregon State University Tidal Inversion Software) regional tidal solution for the U.S. East Coast (1/30º×1/30º) are used to calculate the M_2 amplitude from HA and EMD methods. The model assimilated Topex/Poseidon, Topex Tandem and ERS data. The M_2 amplitudes are generated with the Oregon State University Tidal Prediction Software (OTPS, Egbert and Everofeva, 2002) and listed in Table 1. Although half of the sites are out of the model grid or on land, high agreements are observed between EMD/HA and model derived M_2 tide amplitudes. At Eastport, M_2 amplitudes of 2.64 m, 2.75 m and 2.77m are obtained from the HA, EMD and model solution, respectively. Notes high discrepancies at Lewes and Sewells Point may attribute to the locations of the sites.

4. Discussion and summary

The EMD/HHT has been widely used for various geophysical data. The HA is one of the most popular method to investigate the changes in tidal properties (e.g., Mawdsley et al., 2015). This study is possibly the first test that tries to adopt the EMD technique to describe the M_2 amplitude variability using the hourly tide gauge records; the results show high consistency with the results estimated with the HA method and the independent OTIS regional tidal solution for the U.S. east coast. Compared with HA, the advantage of the EMD over fitting methods is that it is more general and can systematically filter out oscillating modes with unknown and variable frequencies. Also, there is no need to perform multiple HA calculations on small subsections (which reduce the accuracy compared with calculations of longer records), and instead, the whole record is analyze at once. The EMD could also provide additional information on the frequency of storm surges or other variations in sea level on different time scales from weekly to decadal, though here only the highest modes relating to the main tidal cycles where analyzed.

The difference between the EMD and HA derived M_2 amplitude evolution is dominated by the nodal cycle, which is captured by the EMD analysis mode 1. The nodal cycle significant contribute to regional coastal changes (e.g., Gratiot et al., 2008) and impact coastal high tidal levels (Haigh et al., 2011). Accounting of global median amplitude of 2.2 cm nodal cycle is crucial to accurately estimate regional SLR (Baat et al., 2012). The EMD method demonstrates nodal cycle modulations of about 2-3% (e.g., 1 - 6cm) of M_2 tide amplitude at the selected tide gauges along the U.S east coast. The magnitude is consistent with findings based on equilibrium tide expectation (Fig. 1b of Haigh et al., 2011). The comparison implies that indeed, the long nodal cycle can affect tidal analysis if not explicitly removed.

Since the extremely slow changes of the astronomical forcing, tides are usually thought of as stationary (Jay, 2009). So changes in tidal characteristics over time are usually associated with local changes in morphology and tidal currents. In most cases, the changes are not fully understood and may be region-dependent (Woodworth, 2010), as the physical processes cause the tidal variations are complicated (Ray, 2006; 2009), particularly along the coast and on the continental shelves (Müller, 2011; 2012). In addition to morphological changes and SLR that affect the propagation pattern of tidal currents (which depend on water depth and the shape of coastlines and bays), the changes in mixed layer depth caused by the warming of the upper ocean layer may induce additional unknown baroclinic changes in currents. In the Gulf of Maine for example, some small changes in topography or water properties can cause significant changes in the large tides due to the high resonant state of the M_2 tide (Greenberg et al., 2012; Mawdsley et al., 2015).

The Chesapeake and Delaware Bays show high rates of relative SLR (Ezer and Corlett, 2012; Ezer and Atkinson, 2014) and they have very different tidal characteristics than the Gulf of Maine. The uneven vertical land subsidence (-1.90 mm/yr at Kiptopeke, -1.33 mm/yr at Chesapeake City and Baltimore, -2.61 mm/yr at Sewells Point and up to -3.34 at Chesapeake Bay Bridge Tunnel; (Zervas et al., 2013) contributes to uneven local SLR rates (Santamaría-Gómez et al., 2012). In addition, the shape of estuaries and bays can affect the change in tidal amplitude, as shown by the numerical simulations of Lee et al. (2016), who concluded that tidal ranges and tidal energy in Delaware Bay and Chesapeake Bay will change differently under higher sea levels when low-lying regions (5 m) are allowed to flood. The changes of estuarine geometry and high sea levels may be responsible to the observed M_2 amplitude decrease in the lower Chesapeake Bays (Kiptopeake to Sewells Point in Figure 3), which are in agreement with the numerical experiments in Lee et al. (2016).

At Wilmington, both HA and EMD analysis demonstrate similar significant increase in the M_2 amplitude due to morphological changes at the river where the tide gauge is located, as previously reported (Ezer and Atkinson, 2014). Consistent with the study of Müller (2011), in the South Atlantic Bight, the M_2 tidal amplitude increased at Charleston until ~1980 and then remains flat (Ray, 2006). The other two tide gauges (Fort Pulaski and Fernandina) also show notable M_2 amplitude variability with a negative offset after 1980 with the removal of trend during 1930-1980, which might be associated with response to decadal variability in the Atlantic Ocean. The vertical land subsidence is also notable at the sites (-1.24 mm/yr at Charleston, -1.36 mm/yr at Pulaski, -0.60 mm/yr at Fernandina from tide gauge records in the period from the starring year to 2006, (Zervas et al., 2013)). In Miami Beach, Florida, tidal flooding events increased by more than 400% after 2006 (Wdowinski et al., 2016). Hence, the variability of tides should be considered in future regional sea level projections and evaluation of flood risks, since an increase in tidal amplitude (by either sea level rise or local morphology change) would increase the risk of tidal flooding (Ezer and Atkinson, 2014). Furthermore, changes in the tide should not be neglected for implementing sea level rise mitigation and adaptation measures.

Global changes in tidal properties may have large spatial variations since different mechanisms may dominate different coasts. Recent studies highlight the fact that tidal propagation in shallow waters are modified by mean SLR, intensifying coastal threats at some locations (e.g., Li et al., 2016). Furthermore, Müller et al. (2011) lists other possible reasons for the tidal trend, e.g., variations in atmospheric dynamics and changes in the ocean circulation. The bathymetric changes, e.g., increased depth and width caused by dredging and channel modification, can cause long-term changes to the magnitudes of storm tides within harbors and Estuaries (Orton et al., 2015). In New York Harbor (e,g, the Battery station), significant change in storm tide magnitudes have occurred since 1840s. It is attributes to local changes to bathymetry and the interannual variability in storm tides, which anticorrelated with NAO (North Atlantic Oscillation) index (Talke et al., 2014). At Wilmington, increased channel depths are the primary cause of altered tide range (Familkhalili and Talke, 2016).

The variations in AMOC and the GS contribute to the regional sea level variations on multi time scales (e.g., Ezer, 2015; Ezer et al., 2013, 2016; Hakkinen, 2001; Han et al., 2016; Lorbacher et al., 2010; Yin and Goddard, 2013), so a period of months to few years of higher than normal sea level can also be accompanied by interannual variations in tidal amplitudes, as seen here. Variations in GS transport produce variations in sea level gradient across the entire GS length and this large-scale signal is then transmitted into the shelf by the generation of coastal-trapped waves (Ezer, 2016). However, the exact mechanism of how changes in offshore currents such as the GS and changes in wave field may affect the tidal variability over the different regions, will require further research.

Acknowledgement

This study was supported by Old Dominion University's Climate Change and Sea Level Rise Initiative (CCSLRI), the National Natural Science Foundation of China, China (Grants No. 41306194 and 41576168), the Priority Academic Program Development of Jiangsu Higher Education Institutions (Marine Science). The hourly tide gauge data is available from http://opendap.co-ops.nos.noaa.gov/dods/IOOS/. We are thankful to G. D. Egbert and S. Y. Everofeva for providing the OTIS regional tidal solution for the U.S. East Coast (http://volkov.oce.orst.edu/tides/EC.html) and Oregon State University Tidal Prediction Software

(OTPS, http://volkov.oce.orst.edu/tides). Two anonymous reviewers are thanked for providing many useful suggestions that greatly improved the paper.

Appendix

Figure A1 here

Figure A2 here

References

Atkinson, L. P., T. Ezer, and E. Smith, 2013: Sea level rise and flooding risk in Virginia, *Sea Grant Law Policy J.*, **5(2)**, 3-14.

Baart, F., P. H. Van Gelder, J. De Ronde, M. Van Koningsveld, & B. Wouters, 2011: The effect of the 18.6-year lunar nodal cycle on regional sea-level rise estimates. *J. Coastal Res.*, **28(2)**, 511-516.

Bell, C., J. M. Vassie, and P. L. Woodworth, 1996: The Tidal Analysis Software Kit (TASK Package). TASK-2000 version dated December 1998. Available from www. psmsl.org.

Bonaduce, A., N. Pinardi, P. Oddo, G. Spada, G. Larnicol, 2016: Sea-level variability in the Mediterranean Sea from altimetry and tide gauges. *Clim. Dyn.*, doi:10.1007/s00382-016-3001-2.

Cheng, Y., T. Ezer, and B. D. Hamlington, 2016: Sea Level Acceleration in the China Seas. *Water*, **8**, 293.

Church, J. A., and N. J. White, 2011: Sea-level rise from the late 19th to the early 21st century. *Surv. Geophys.*, **32**, 585-602, doi:10.1007/s10712-011- 9119-1.

Codiga, D. L., 2011: Unified Tidal Analysis and Prediction Using the UTide Matlab Functions, *Technical Report 2011-01*, Graduate School of Oceanography, University of Rhode Island, Narragansett, RI. 59pp. ftp://www.po.gso.uri.edu/pub/downloads/codiga/pubs/2011Codiga-UTide-Report.pdf

Ezer, T., 2015: Detecting changes in the transport of the Gulf Stream and the Atlantic overturning circulation from coastal sea level data: The extreme decline in 2009-2010 and estimated variations for 1935-2012. *Glob. Planet. Change*, **129**, 23-36, doi:10.1016/j.gloplacha.2015.03.002.

-----, 2016: Can the Gulf Stream induce coherent short-term fluctuations in sea level along the US East Coast? A modeling study. *Ocean dynam.*, **66**, 207-220. DOI 10.1007/s10236-016-0928-0.

-----, I. D. Haigh, and P. L. Woodworth, 2016: Nonlinear sea-level trends and long-term variability on western European coasts. *J. Coastal Res*., **32(4),** 744-755, doi:10.2112/JCOASTRES-D-15-00165.1.

-----, and L. P. Atkinson, 2014: Accelerated flooding along the U.S. East Coast: On the impact of sea-level rise, tides, storms, the Gulf Stream, and the North Atlantic Oscillations. *Earth's Future*, **2**, 362–382. doi:10.1002/2014EF000252

-----, and W. B. Corlett, 2012: Is sea level rise accelerating in the Chesapeake Bay? A demonstration of a novel new approach for analyzing sea level data. *Geophys. Res. Lett*., **39**, L19605, doi:10.1029/2012GL053435.

-----, L. P. Atkinson, W. B. Corlett, and J. L. Blanco, 2013: Gulf Stream's induced sea level rise and variability along the U.S. mid-Atlantic coast. *J. Geophys. Res. Oceans*, **118(2)**, 685-697. doi:10.1002/jgrc.20091.

Familkhalili, R., and S. Talke, 2016: The effect of channel deepening on tides and storm surge: A case study of Wilmington, NC. *Geophys. Res. Lett*., **43(17)**, 9138-9147.

Flick, R. E., J. F. Murray, and L. C. Ewing, 2003: Trends in United States datum statistics and tide range. *J. Waterw. Port Coastal Ocean Eng*., **129**, 155-164.

Foreman, M. G. G., 1977: Manual for tidal heights analysis and prediction. *Pac. Mar. Sci. Rep*., **77-10**, 58 pp., Inst. of Ocean Sci., Sidney, B. C., Canada.

Egbert, G. D. and S. Y. Erofeeva, 2002: Efficient inverse modeling of barotropic ocean tides. *Journal Atmos. Oceanic Technol*., **19**, 183204. doi: http://dx.doi.org/10.1175/1520¬0426(2002)019<0183:EIMOBO>2.0.CO;2

Gratiot, N., E. J. Anthony, A. Gardel, C. Gaucherel, C. Proisy, and J. T. Wells 2008: Significant contribution of the 18.6 year tidal cycle to regional coastal changes. *Nat. Geosci*., **1(3)**, 169-172.

Greenberg, D. A., W. Blanchard, B. Smith, and E. Barrow, 2012: Climate Change, Mean Sea Level and High Tides in the Bay of Fundy. *Atmos.-Ocean*, **50(3)**, 261-276. doi:10.1080/07055900.2012.668670

Hakkinen, S., 2001: Variability in sea surface height: a qualitative measure for the meridional overturning in the North Atlantic. *J. Geophys. Res*., **106**, 13837-13848.

Han, W., G. A. Meehl, D. Stammer, A. Hu, B. Hamlington, J. Kenigson, H. Palanisamy, and P. Thompson, 2016: Spatial patterns of sea level variability associated with natural internal climate modes, *Surv. Geophys*., 1-34. doi: doi:10.1007/s10712-016-9386-y

Haigh, I. D., M. Eliot, and C. Pattiaratchi, 2011: Global influences of the 18.61 year nodal cycle and 8.85 year cycle of lunar perigee on high tidal levels. *J. Geophys. Res*., **116**, C06025, doi:10.1029/2010JC006645.

Houston, J. R., and R. G. Dean, 2011: Sea-level acceleration based on U.S. tide gauges and extensions of previous global-gauge analyses. *J. Coast. Res*., **27(3)**, 409-417

Huang, N. E., Z. Shen, S. R. Long, M. C. Wu, E. H. Shih, Q. Zheng, C. C. Tung, and H. H. Liu, 1998: The empirical mode decomposition and the Hilbert spectrum for non-stationary time series analysis. *Proc. R. Soc. London Ser. A*, **454**, 903-995.

Huang, N. E., and Z. Wu, 2008: A review on Hilbert-Huang transform: the method and its applications on geophysical studies. *Rev. Geophys*., **46**, RG2006.

Jay, D. A., 2009: Evolution of tidal amplitudes in the eastern Pacific Ocean. *Geophys. Res. Lett*., **36(4)**, L04603, doi:10.1029/2008Gl036185

Karegar, M. A., T. H. Dixon, and S. E. Engelhart, 2016: Subsidence along the Atlantic Coast of North America: Insights from GPS and late Holocene relative sea level data. *Geophys. Res. Lett*., **43**, doi:10.1002/2016GL068015.

Kopp, R. E., 2013: Does the mid-Atlantic United States sea-level acceleration hot spot reflect ocean dynamic variability? *Geophys. Res. Lett*., **40**, 3981-3985, doi:10.1002/GRL.50781

Lee, S. B., M. Li, and F. Zhang., 2016: The effect of sea level rise on Tidal Dynamics in Chesapeake and Delaware Bays, *Ocean Sciences Meeting 2016*, EC31A-06, ,21-26 February, New Orleans, Louisiana, USA. https://agu.confex.com/agu/os16/preliminaryview.cgi/Paper93354.html

Li, Y., H. Zhang, C. Tang, T. Zou, and D. Jiang, 2016: Influence of Rising Sea Level on Tidal Dynamics in the Bohai Sea. *J. Coastal Res*., **74(sp1)**, 22-31.

Lorbacher, K., J. Dengg, C.W. Böning, A. Biastoch, 2010: Regional patterns of sea level change related to interannual variability and multidecadal trends in the Atlantic meridional overturning circulation. *J. Clim*., **23(15)**, 4243-4254. http://dx.doi.org/10.1175/2010JCLI3341.1.

Mawdsley, R. J., I. D. Haigh, and N. C. Wells, 2015: Global secular changes in different tidal high water, low water and range levels. *Earth's Future*, **3**, 66-81. doi:10.1002/2014EF000282.

Müller, M., 2011: Rapid change in semi-diurnal tides in the North Atlantic since 1980. *Geophys. Res. Lett*., **38**, L11602, doi:10.1029/2011GL047312

Müller, M., H. Haak, J. H. Jungclaus, J. Sündermann, and M. Thomas, 2010: The effect of ocean tides on a climate model simulation. *Ocean Model.*, **35(4)**, 304-313. doi:10.1016/j.ocemod.2010.09.001

-----, B. K. Arbic, and J. X. Mitrovica, 2011: Secular trends in ocean tides: Observations and model results. *J. Geophys. Res*., **116**, C05013, doi:10.1029/2010JC006387.

Orton, P., S. Talke, D. Jay, L. Yin, A. Blumberg, N. Georgas, and K. MacManus, 2015: Channel shallowing as mitigation of coastal flooding. *J. Mar. Sci. Eng*., **3(3)**, 654–673, doi:10.3390/jmse3030654.

Pawlowicz, R., B. Beardsley, and S. Lentz, 2002: Classical tidal harmonic analysis including error estimates in MATLAB using TDE. *Comput. Geosci.*, **28(8)**, 929-937. doi:10.1016/S0098-3004(02)00013-4.

Pelling, H. E., J. A. Mattias Green, and S. L. Ward, 2013: Modelling tides and sea-level rise: To flood or not to flood. *Ocean Model.*, 63, 21-29. doi:10.1016/j.ocemod.2012.12.004.

Ray, R. D., 2006: Secular changes of the M2 tide in the Gulf of Maine. *Cont. Shelf Res*., **26**, 422-427. doi:10.1016/j.csr.2005.12.005.

-----, 2009: Secular changes in the solar semidiurnal tide of the western North Atlantic Ocean, *Geophys. Res. Lett*., **36**, L19601. doi:10.1029/2009GL040217.

Sallenger, A. H., K. S. Doran, and P. Howd, 2012: Hotspot of accelerated sea-level rise on the Atlantic coast of North America. *Nat. Clim. Change,* **24**, doi:10.1038/NCILMATE1597

Santamaría-Gómez, A., M. Gravelle, X. Collilieux, M. Guichard, B. M. Míguez, P. Tiphaneau, and G. Wöppelmann, 2012: Mitigating the effects of vertical land motion in tide gauge records using a state-of-the-art GPS velocity field. *Global Planet. Change*, **98-99**, 6-17. doi:10.1016/j.gloplacha.2012.07.007

Sha, J., Y.-H. Jo, X.-H. Yan, and W. T. Liu, 2015: The modulation of the seasonal cross-shelf sea level variation by the cold pool in the Middle Atlantic Bight. *J. Geophys. Res. Oceans*, **120**, 7182-7194, doi:10.1002/2015JC011255.

Sweet, W. V. and J. Park, 2014: From the extreme to the mean: Acceleration and tipping points of coastal inundation from sea level rise. *Earth's Future*, **2(12)**, 579-600.

Talke, S. A., P. Orton, and D. A. Jay, 2014: Increasing storm tides in New York Harbor, 1844-2013. *Geophys. Res. Lett*., **41**, 3149-3155, doi:10.1002/2014GL059574.

Tebaldi, C., B. H. Strauss, and C. E. Zervas, 2012: Modelling sea level rise impacts on storm surges along US coasts. *Environ. Res. Lett*., **7**, 014032.

Wahl, T., F. M. Calafat, and M. E. Luther, 2014: Rapid changes in the seasonal sea level cycle along the US Gulf coast from the late 20th century. *Geophys. Res. Lett*., **41**, 491-498.

Wdowinski, S., R. Bray, B. P. Kirtman, and Z. Wu, 2016: Increasing flooding hazard in coastal communities due to rising sea level: Case study of Miami Beach, Florida. *Ocean Coast. Manage.*, **126**, 1-8. doi:10.1016/j.ocecoaman.2016.03.002

Woodworth, P. L., 2010: A survey of recent changes in the main components of the ocean tide. *Cont. Shelf Res*., **30(15)**, 1680-1691. doi:10.1016/j.csr.2010.07.002

-----, 2011: A note on the nodal tide in sea level records. *J. Coastal Res*., **28**, 316-323, doi:10.2112/jcoastres-d-11a-00023.1.

Yin, J., Goddard, P.B., 2013: Oceanic control of sea level rise patterns along the East Coast of the United States. *Geophys. Res. Lett*., **40**, 5514-5520. http://dx.doi.org/10.1002/2013GL057992.

Zervas, C., S. Gill, and W. Sweet, 2013: Estimating vertical land mothion from long-term tide gauge records, *NOAA technical report*, technical Report NOS CO-OPS 065, https://tidesandcurrents.noaa.gov/publications/Technical_Report_NOS_CO-OPS_065.pdf

Zhang, K., 2011: Analysis of non-linear inundation from sea-level rise using LIDAR data: A case study for south Florida. *Clim. Change*, 106, 535-565, doi:10.1007/s10584-010-9987-2.

Zhang, H., and J. Sheng, 2013: Estimation of extreme sea levels over the eastern continental shelf of North America. *J. Geophys. Res. Oceans*, **118**, 6253-6273, doi:10.1002/2013JC009160.

Captions:

Table 1. Details of the selected Hourly Sea-Level Data (CBBT: Chesapeake Bay Bridge Tunnel, Norfolk: Sewells Point). For each site, the columns 1-9 are name of the site, latitude (Lat) and longitude (Long), start year of the data (end in 2016), the mean of M2 tide amplitude (Amp., m) estimated using harmonic analysis (HA), mean magnitude of EMD analysis mode 1 (m) and the removed modulation of nodal cycle (Nodal, m) using Eq.(2), M2 tide amplitude (m) estimated from East Coast of America model with the Oregon State University Tidal Prediction Software (OTPS, '*' denotes the site is out of model grid or on land), correlation coefficient between HA and EMD analysis derived variations of M2 tide amplitude (Fig.3) and the mean periods (h) of EMD analysis modes 1 and 2, respectively.

Figure 1. Bathymetry of the study area and location of the selected tide gauges (the numbers according to the tide gauges listed in Table 1). The regions with water depth larger than 1000 m are marked as grey.

Figure 2. (a) Hourly sea level time series estimated with EMD analysis (the first mode, m) at Wilmington. The Black curve denotes the M2 tide amplitude computed with harmonic analysis (UTide). The red curve denotes the sea level magnitude computed as the mean of peak absolutes of EMD first mode. (b) Period (hour) of the sea level EMD analysis first mode. M2 tide period of 12.42 hour is marked in y-label. (c) The difference (black curve, m) between the sea level variation magnitude and M2 amplitude calculated with EMD analysis (mode 1) and HA. The dashed line is the nodal cycle estimated from EMD (mode 1) sea level variation (m) using Eq. (2). (d-e) are similar to (a-c) but at Eastport.

Figure 3. Evolution of M_2 amplitude estimated using harmonic analysis (Black curves) and EMD (red curves) method. The nodal cycle and the mean amplitude over the all available time period at each site have been removed.

Appendix Figure A1. The EMD/HHT analysis for the Baltimore sea level data (mode 1-19, mode 0 denote original tide gauge records).

Appendix Figure A2. Sea level variations of EMD mode 2 and according periods at (a) Eastport and (b) Wilmington. K1 tide period of 23.93 hour is also shown.

Table 1. Details of the selected Hourly Sea-Level Data (CBBT: Chesapeake Bay Bridge Tunnel, Norfolk: Sewells Point). For each site, the columns 1-9 are name of the site, latitude (Lat) and longitude (Long), start year of the data (end in 2016), the mean of M_2 tide amplitude (Amp., m) estimated using harmonic analysis (HA), mean magnitude of EMD analysis mode 1 (m) and the removed modulation of nodal cycle (Nodal, m) using Eq.(2), M_2 tide amplitude (m) estimated from East Coast of America model with the Oregon State University Tidal Prediction Software (OTPS, '*' denotes the site is out of model grid or on land), correlation coefficient between HA and EMD analysis derived variations of M_2 tide amplitude (Fig.3) and the mean periods (h) of EMD analysis modes 1 and 2, respectively.

Name (State)	Lat. (°)	Long. (°)	Start year	HA Amp.	EMD/ Nodal	OTPS (EC)	Correlation (r)	Periods (Mode 1/2)
1. Eastport, ME	44.90	-66.98	1929	2.64	2.75/0.06	2.77	0.94	13.01/24.23
2. Portland, ME	43.66	-70.25	1910	1.35	1.36/0.04	*	0.93	12.62/24.29
3. Boston, MA	42.36	-71.05	1921	1.37	1.43/0.04	*	0.81	13.06/24.17
4. Newport, RI	41.51	-71.33	1930	0.51	0.49/0.02	0.46	0.01	5.89/22.34
5. New London, CT	41.36	-72.09	1938	0.36	0.37/0.01	0.37	0.66	12.89/23.64
6. Battery, NY	40.70	-74.01	1920	0.66	0.67/0.03	0.70	0.89	12.95/23.76
7. Atlantic City, NJ	39.36	-74.42	1911	0.58	0.59/0.02`	0.58	0.30	12.82/23.30
8. Baltimore, MD	39.27	-76.58	1902	0.15	0.11/0.01	*	0.82	10.78/17.61
9. Lewes, DE	38.78	-75.12	1919	0.60	0.61/0.02	0.47	0.76	12.75/24.09
10. Kiptopeke, VA	37.17	-75.99	1976	0.39	0.39/0.01	0.32	0.63	12.56/23.94
11. CBBT, VA	36.97	-76.11	1975	0.38	0.38/0.01	0.30	0.60	12.45/25.56
12. Norfolk, VA	36.95	-76.33	1927	0.36	0.36/0.01	0.21	0.41	12.56/23.96
13. Wilmington, NC	34.23	-77.95	1908	0.58	0.61/0.01	*	1.00	12.97/24.34
14. Charleston, SC	32.78	-79.93	1899	0.77	0.78/0.02	*	0.90	12.72/24.13
15. Fort Pulaski, GA	32.04	-80.90	1935	1.01	1.04/0.03	*	0.79	12.82/24.25
16. Fernandina, WL	30.67	-81.47	1898	0.88	0.90/0.02	*	0.90	12.80/24.28
17. Key West, FL	24.56	-81.81	1913	0.17	0.15/0.01	*	0.58	11.98/20.02

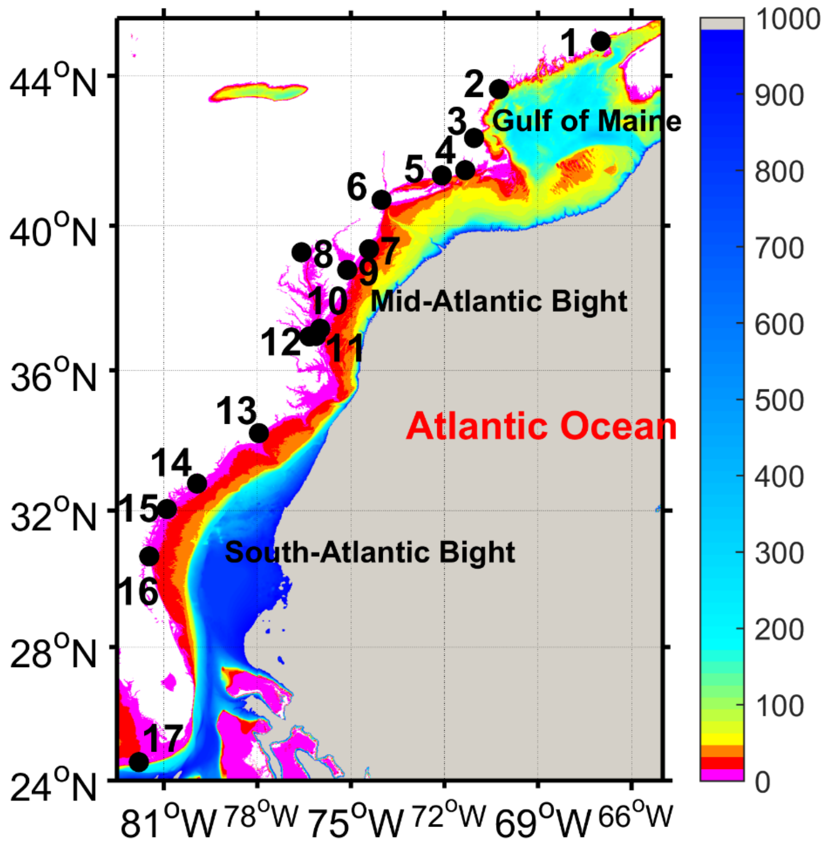

Figure 1. Bathymetry of the study area and location of the selected tide gauges (the numbers according to the tide gauges listed in Table 1). The regions with water depth larger than 1000 m are marked as grey.

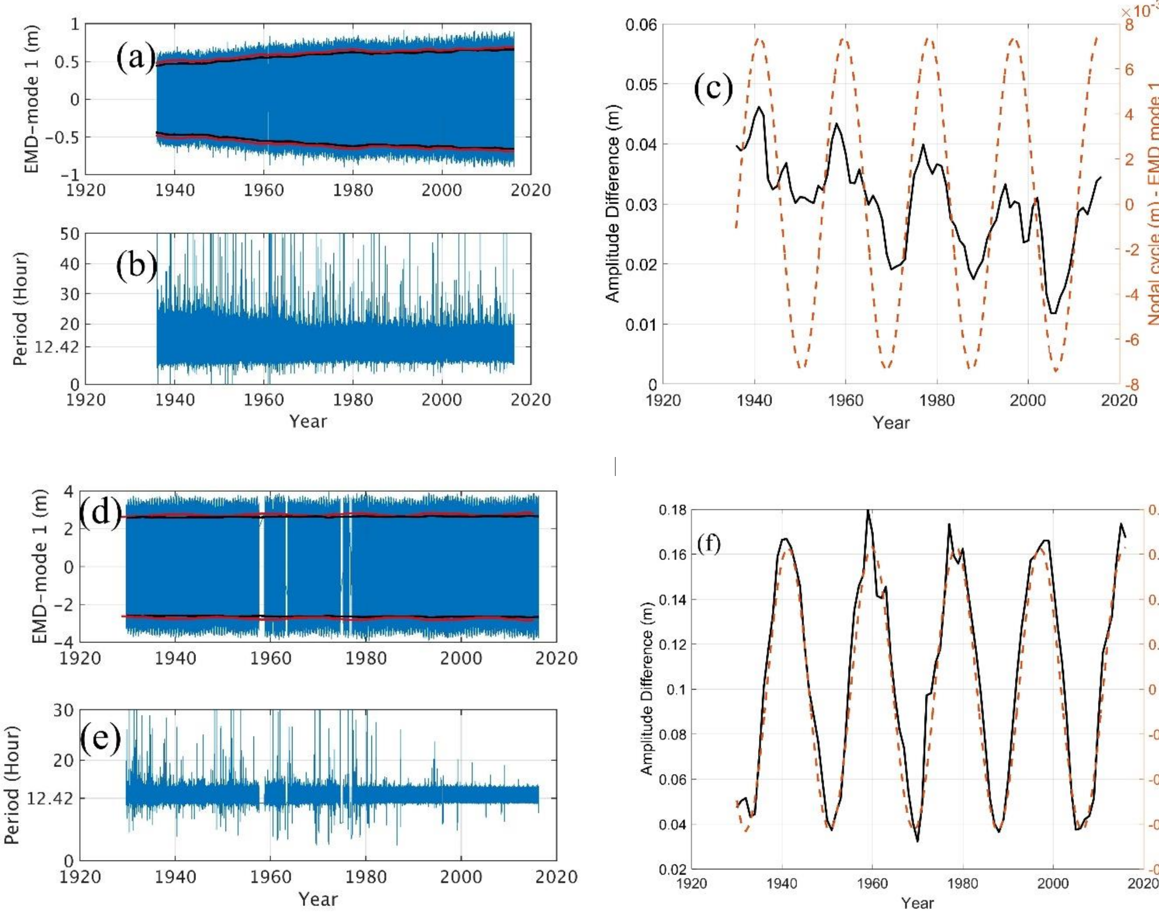

Figure 2. (a) Hourly sea level time series estimated with EMD analysis (the first mode, m) at Wilmington. The Black curve denotes the M2 tide amplitude computed with harmonic analysis (UTide). The red curve denotes the sea level magnitude computed as the mean of peak absolutes of EMD first mode. (b) Period (hour) of the sea level EMD analysis first mode. M2 tide period of 12.42 hour is marked in y-label. (c) The difference (black curve, m) between the sea level variation magnitude and M_2 amplitude calculated with EMD analysis (mode 1) and HA. The dashed line is the nodal cycle estimated from EMD (mode 1) sea level variation (m) using Eq. (2). (d-f) are similar to (a-c) but at Eastport.

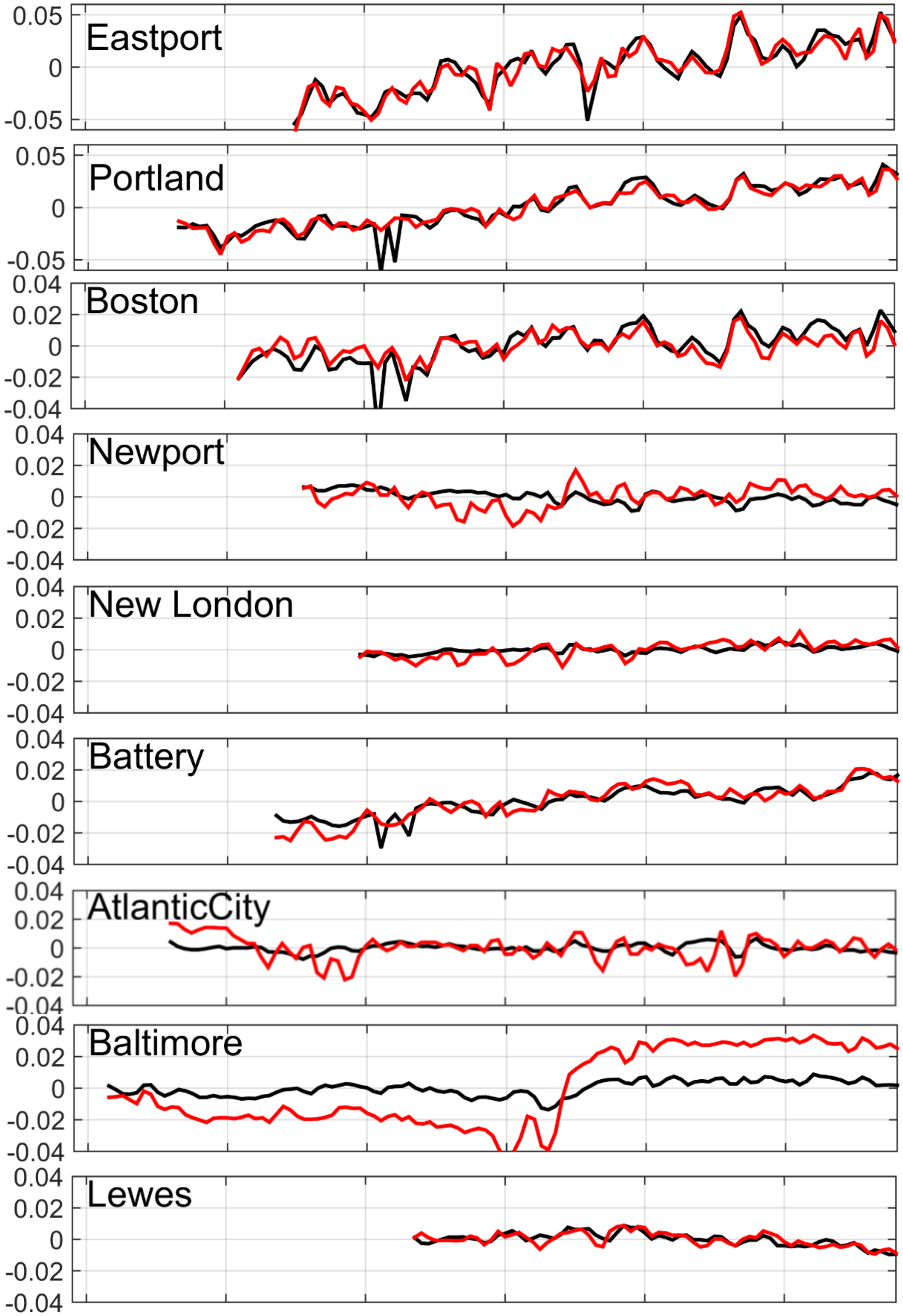
Eastport
0.05
0
-0.05
Portland
0.05
0
-0.05
Boston
0.04
0.02
0
-0.02
-0.04
Newport
0.04
0.02
0
-0.02
-0.04
New London
0.04
0.02
0
-0.02
-0.04
Battery
0.04
0.02
0
-0.02
-0.04
AtlanticCity
0.04
0.02
0
-0.02
-0.04
Baltimore
0.04
0.02
0
-0.02
-0.04
Lewes
0.04
0.02
0
-0.02
-0.04

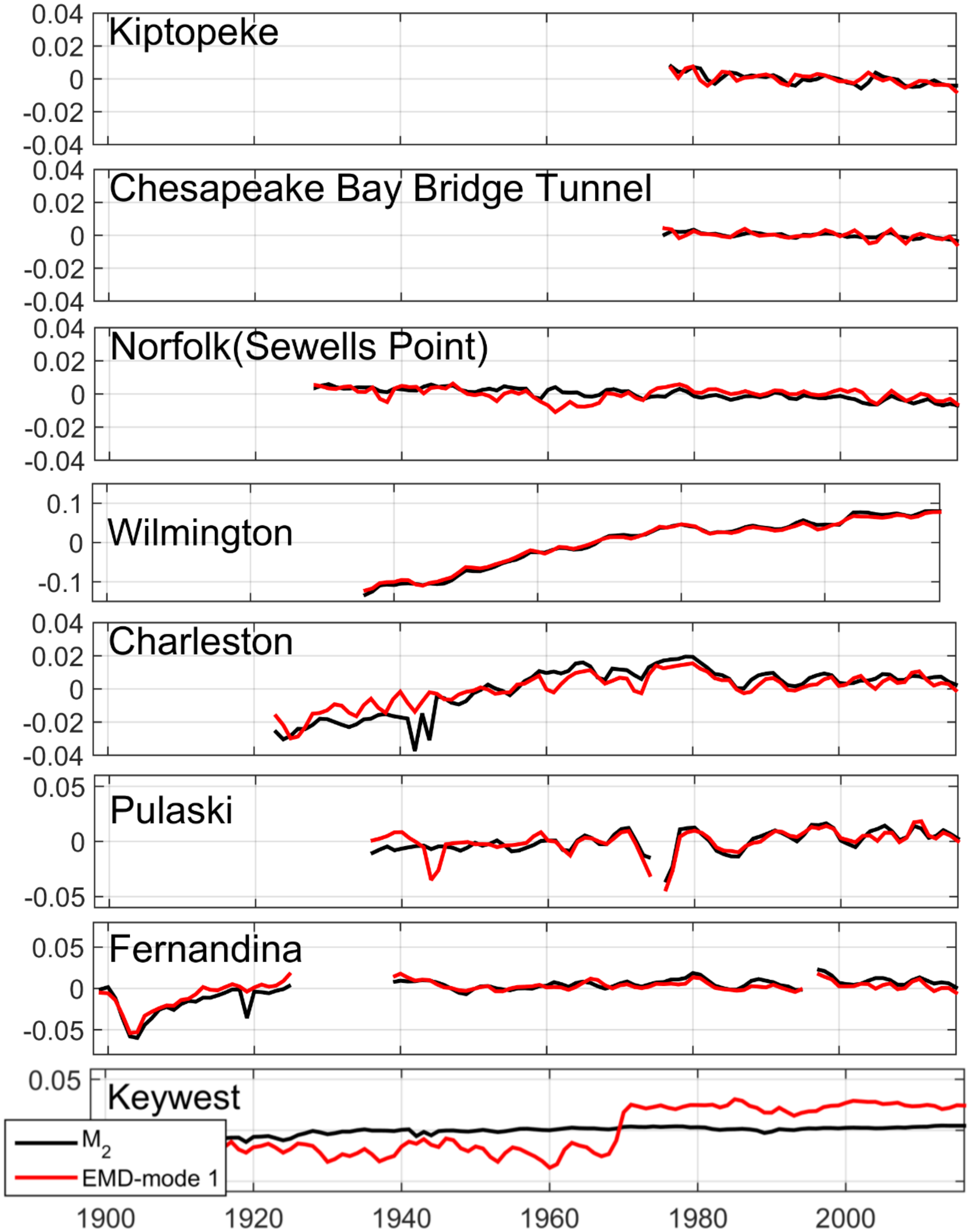

Figure 3. Evolution of M_2 amplitude estimated using harmonic analysis (Black curves) and EMD (red curves) method. The nodal cycle and the mean amplitude over the all available time period at each site have been removed.

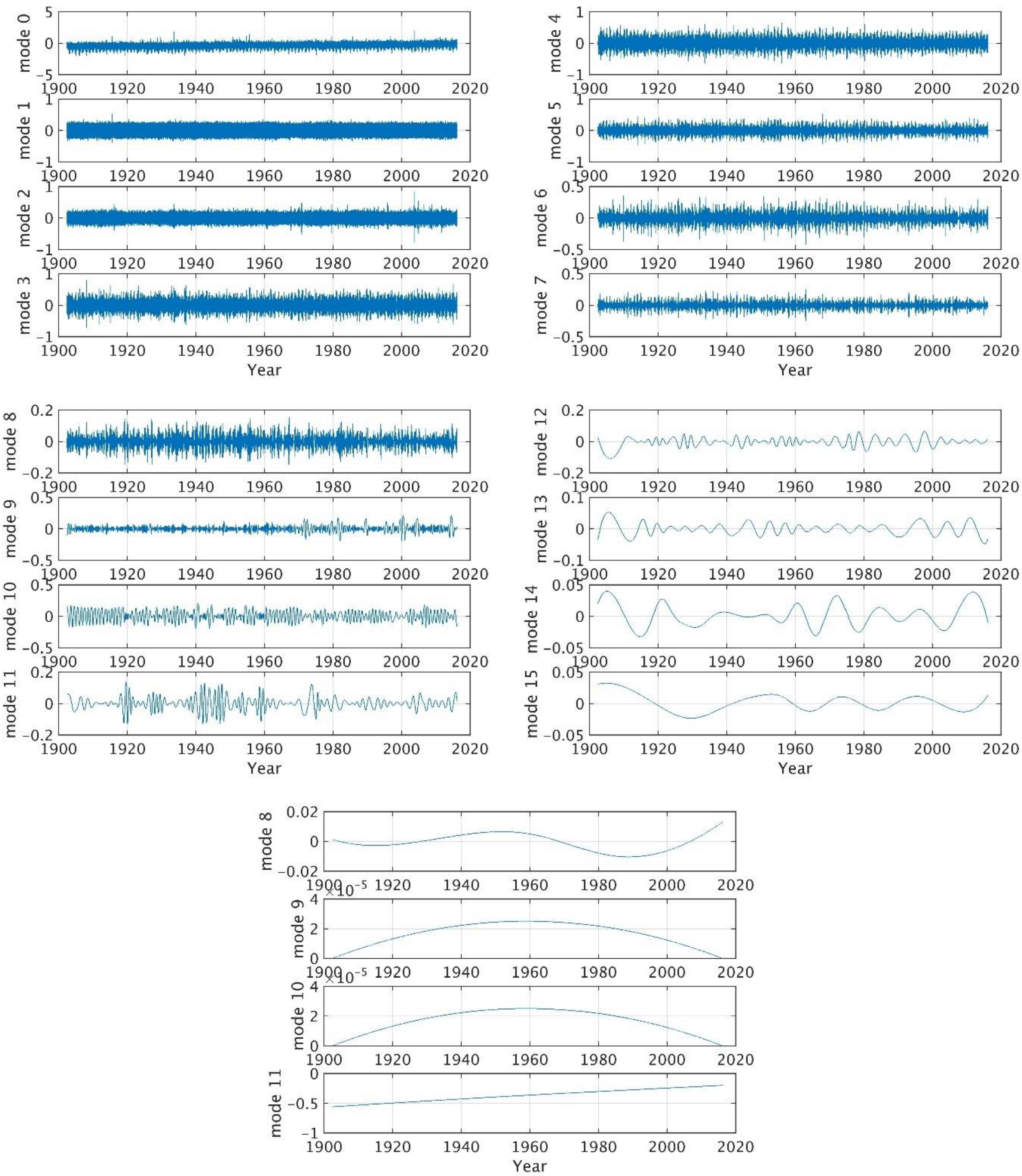

Appendix Figure A1. The EMD/HHT analysis for the Baltimore sea level data (mode 1-19, mode 0 denote original tide gauge records).

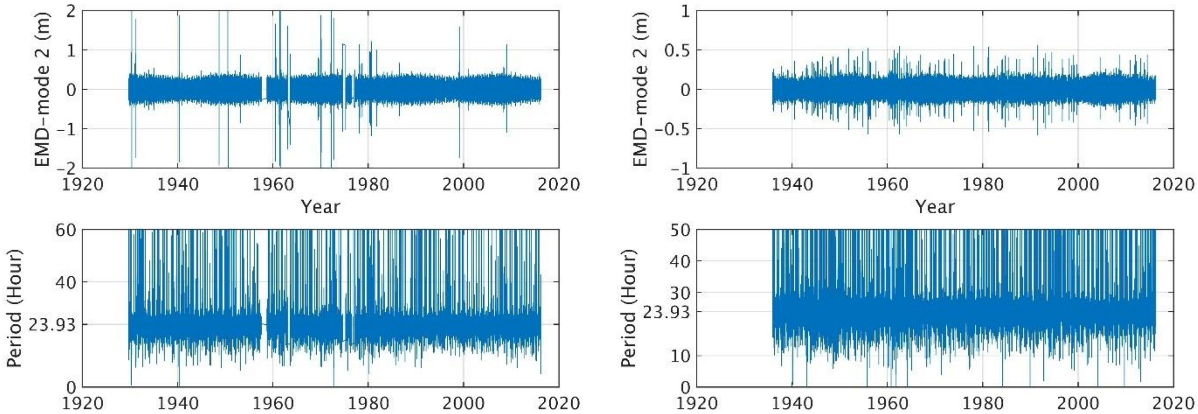

(a) (b)

Appendix Figure A2. Sea level variations of EMD mode 2 and according periods at (a) Eastport and (b) Wilmington. K_1 tide period of 23.93 hour is also shown.

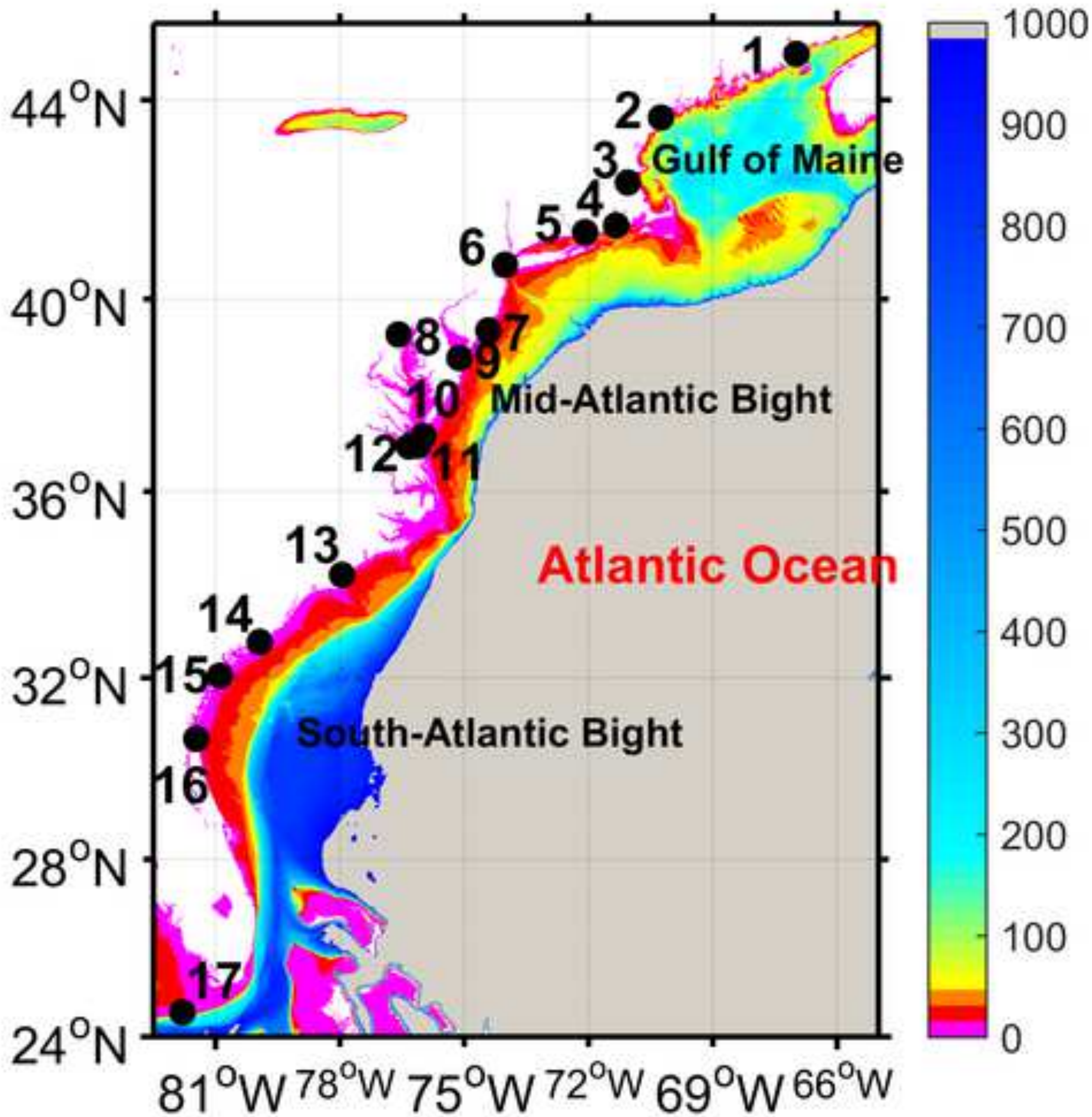
1
2
3
4
5
6
7
8
9
10
11
12
13
14
15
16
17
Gulf of Maine
Mid-Atlantic Bight
Atlantic Ocean
South-Atlantic Bight
44°N
40°N
36°N
32°N
28°N
24°N
81°W
78°W
75°W
72°W
69°W
66°W
1000
900
800
700
600
500
400
300
200
100
0

fig2a-2b

Click here to download Rendered Figure fig2a_2b.jpg

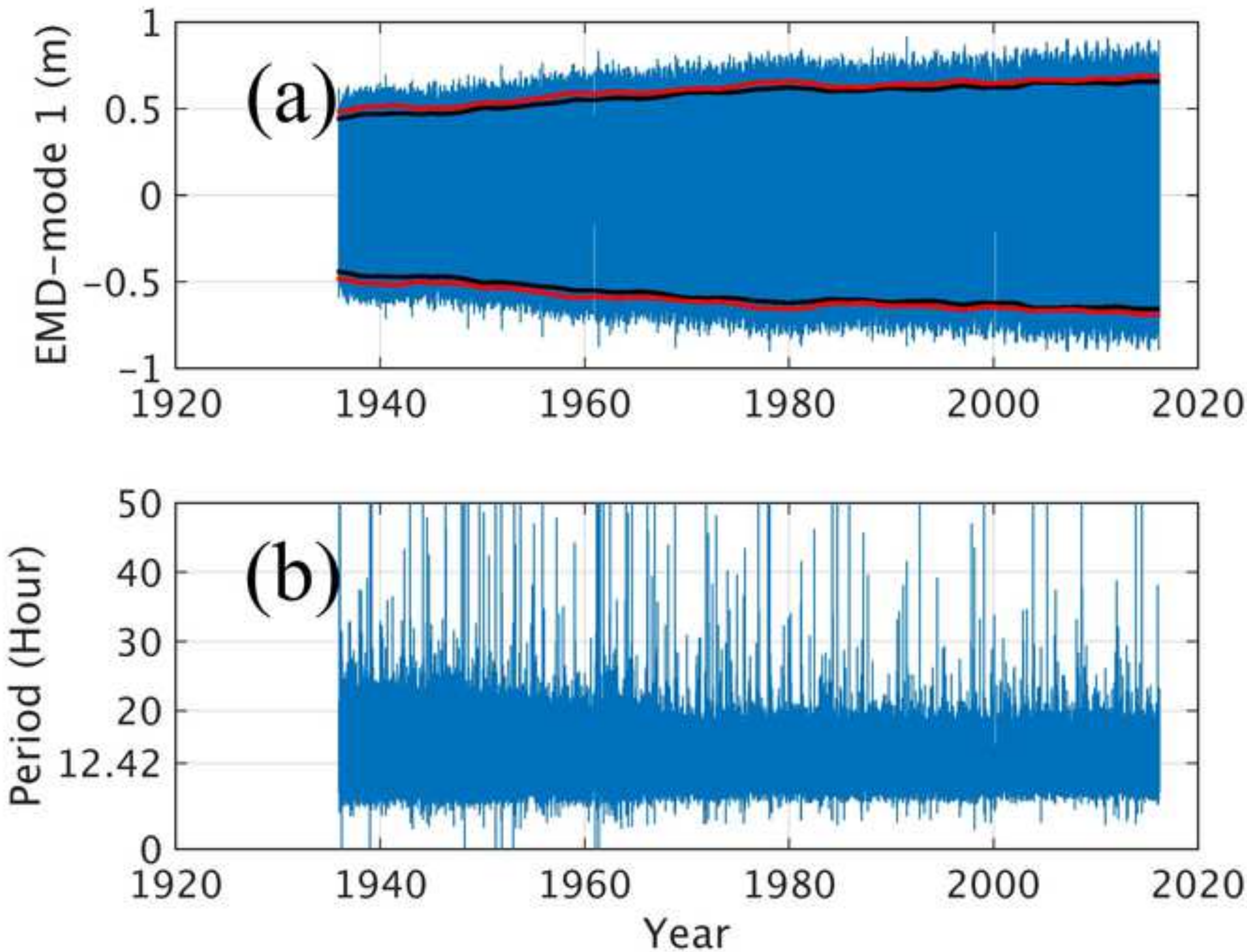

fig2c

Click here to download Rendered Figure fig2c.jpg

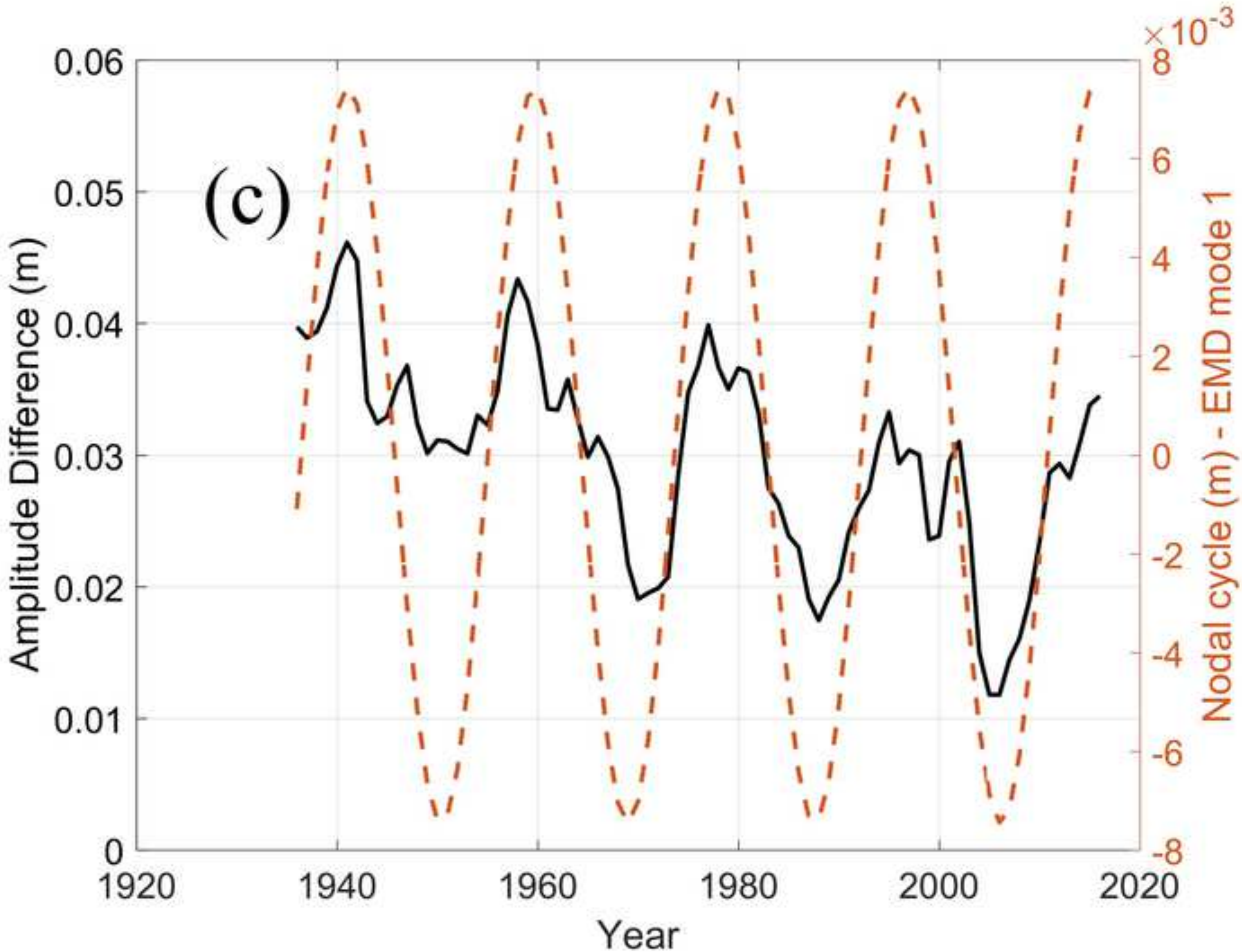

fig2d-2e

Click here to download Rendered Figure fig2d_2e.jpg

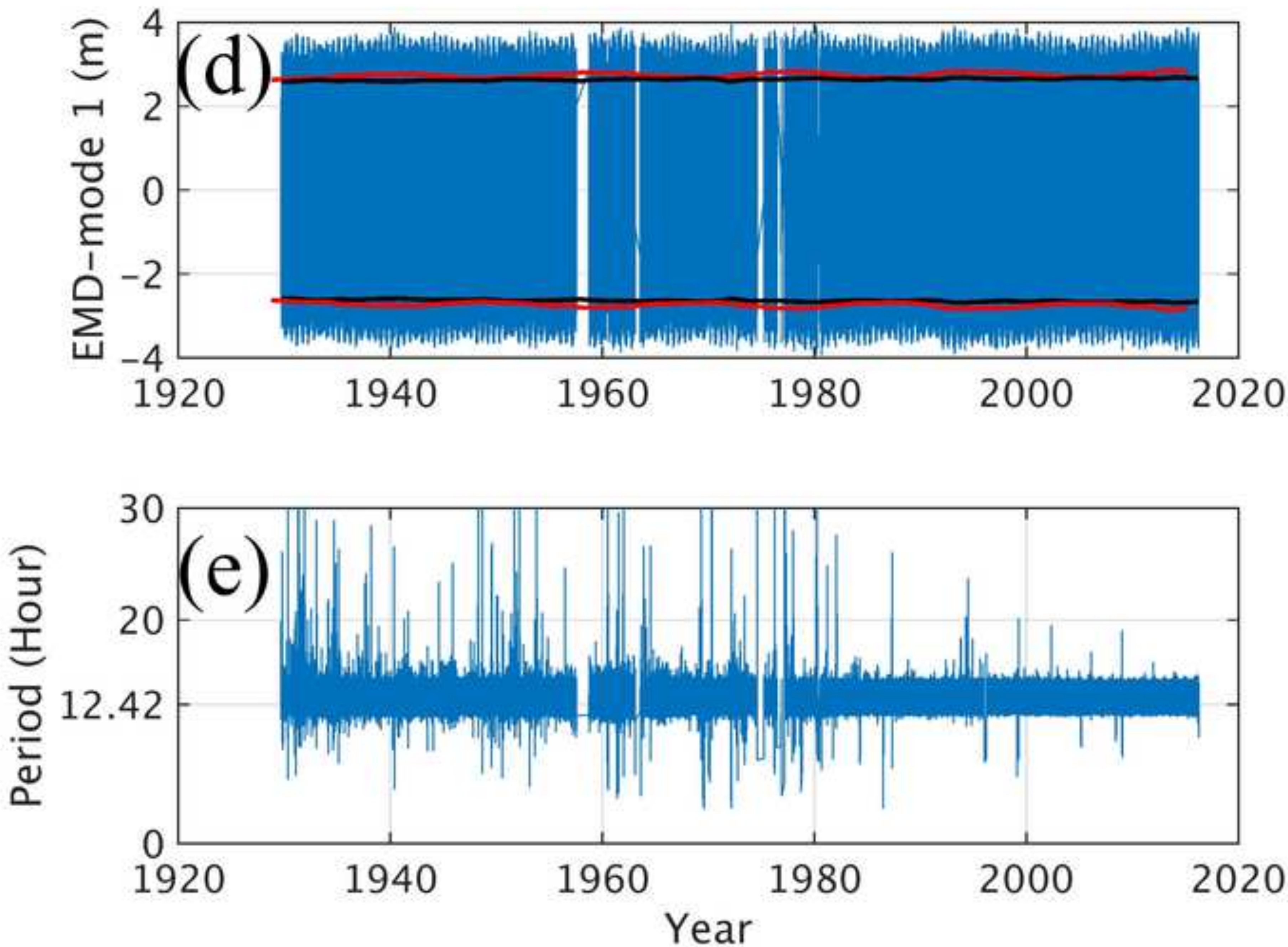

fig2f

Click here to download Rendered Figure fig2f.jpg

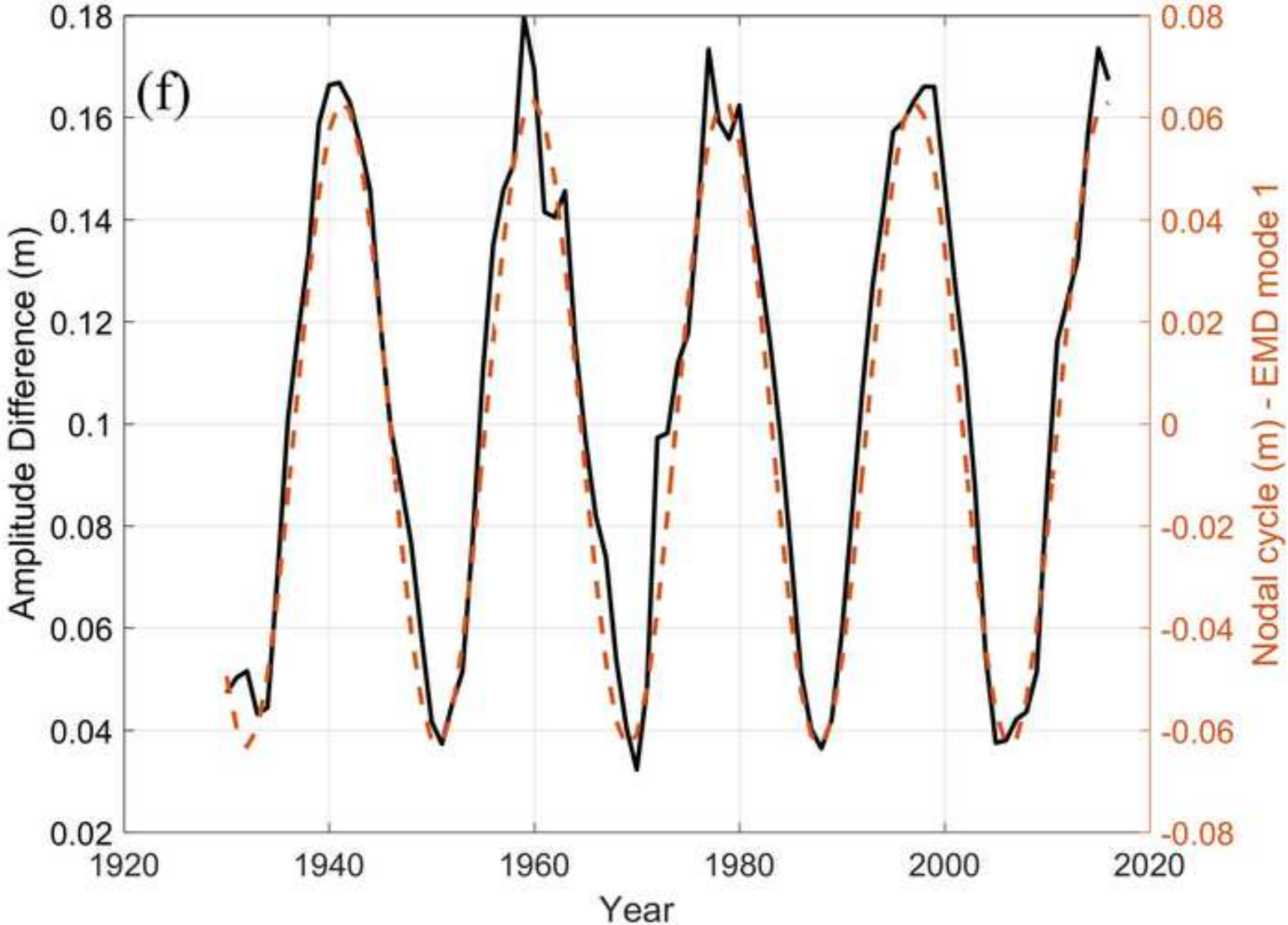

Click here to download Rendered Figure fig3..pdf

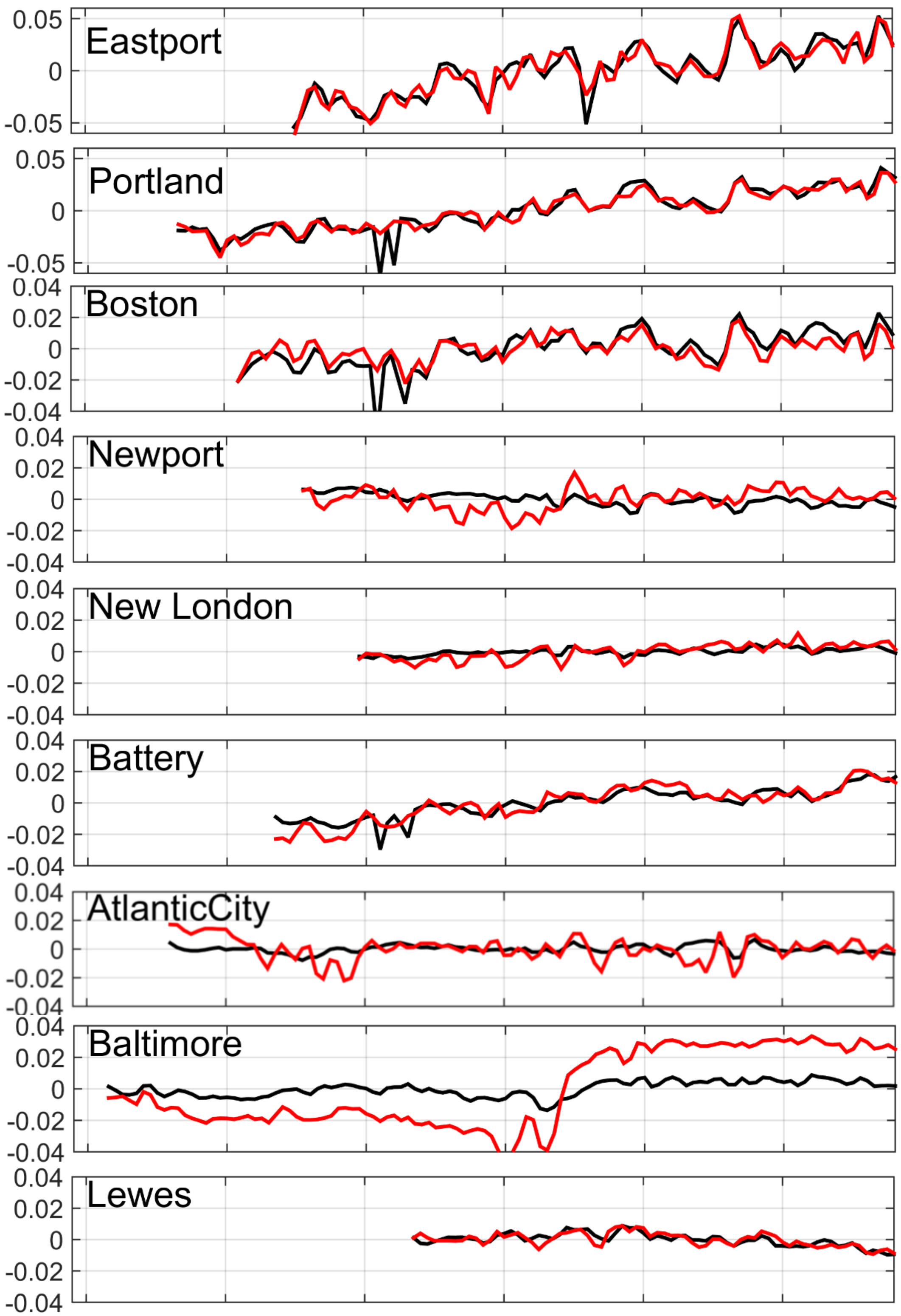

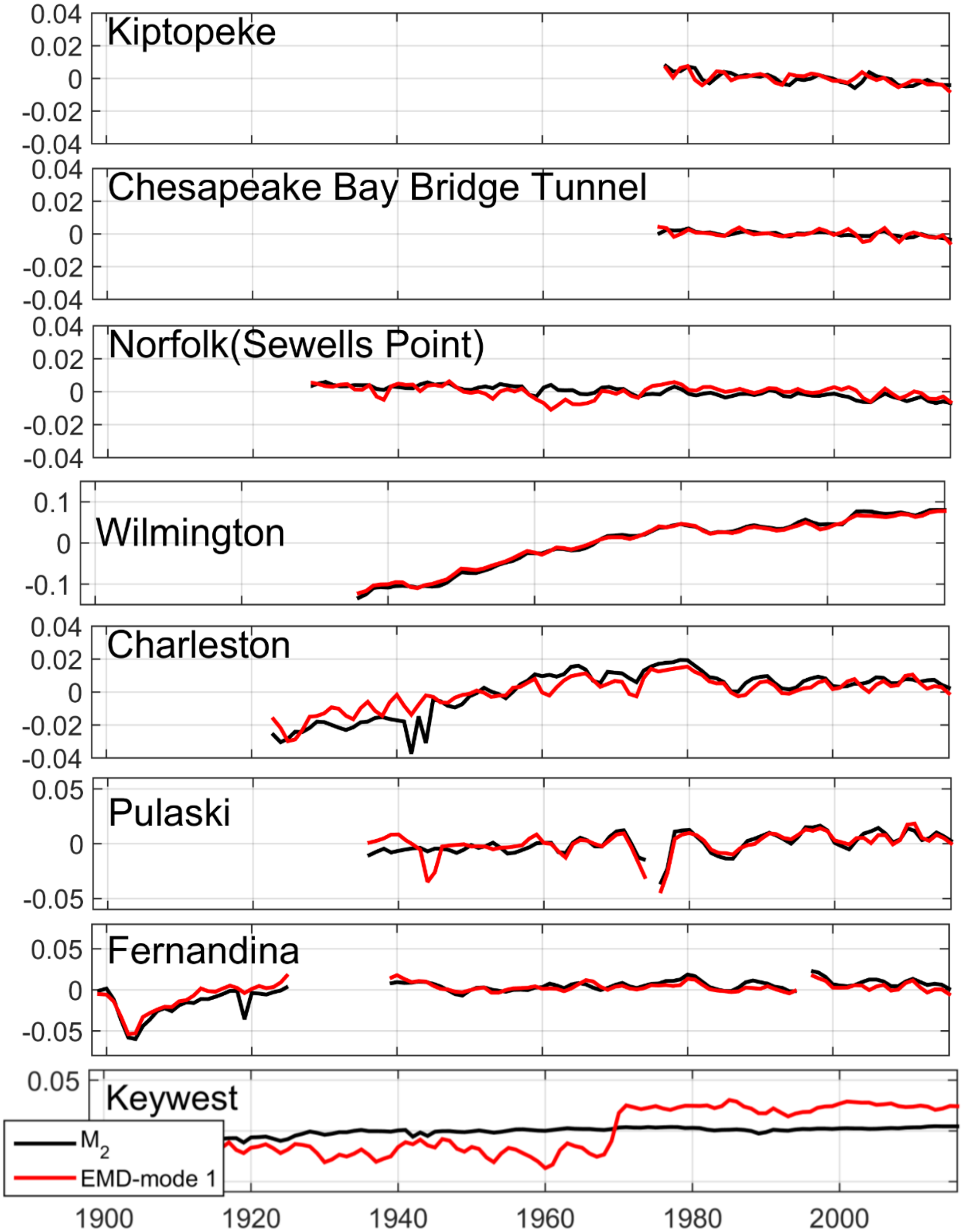
Kiptopeke
Chesapeake Bay Bridge Tunnel
Norfolk(Sewells Point)
Wilmington
Charleston
Pulaski
Fernandina
Keywest
M2
EMD-mode 1
0.04
0.02
0
-0.02
-0.04
0.1
-0.1
0.05
-0.05
1900
1920
1940
1960
1980
2000

figa_a1a

Click here to download Rendered Figure figa_a1a.jpg

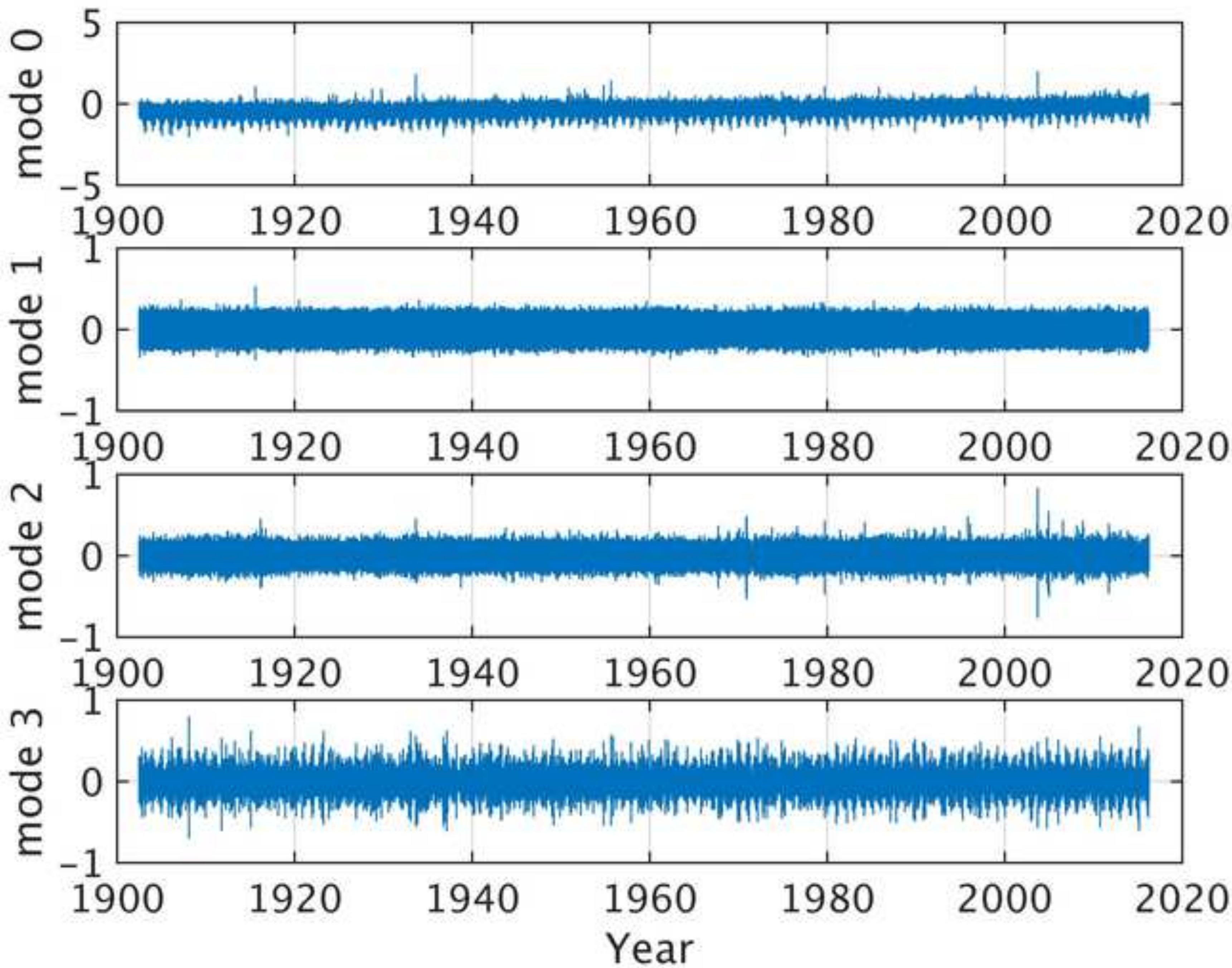

figa_a1b

Click here to download Rendered Figure figa_a1b.jpg

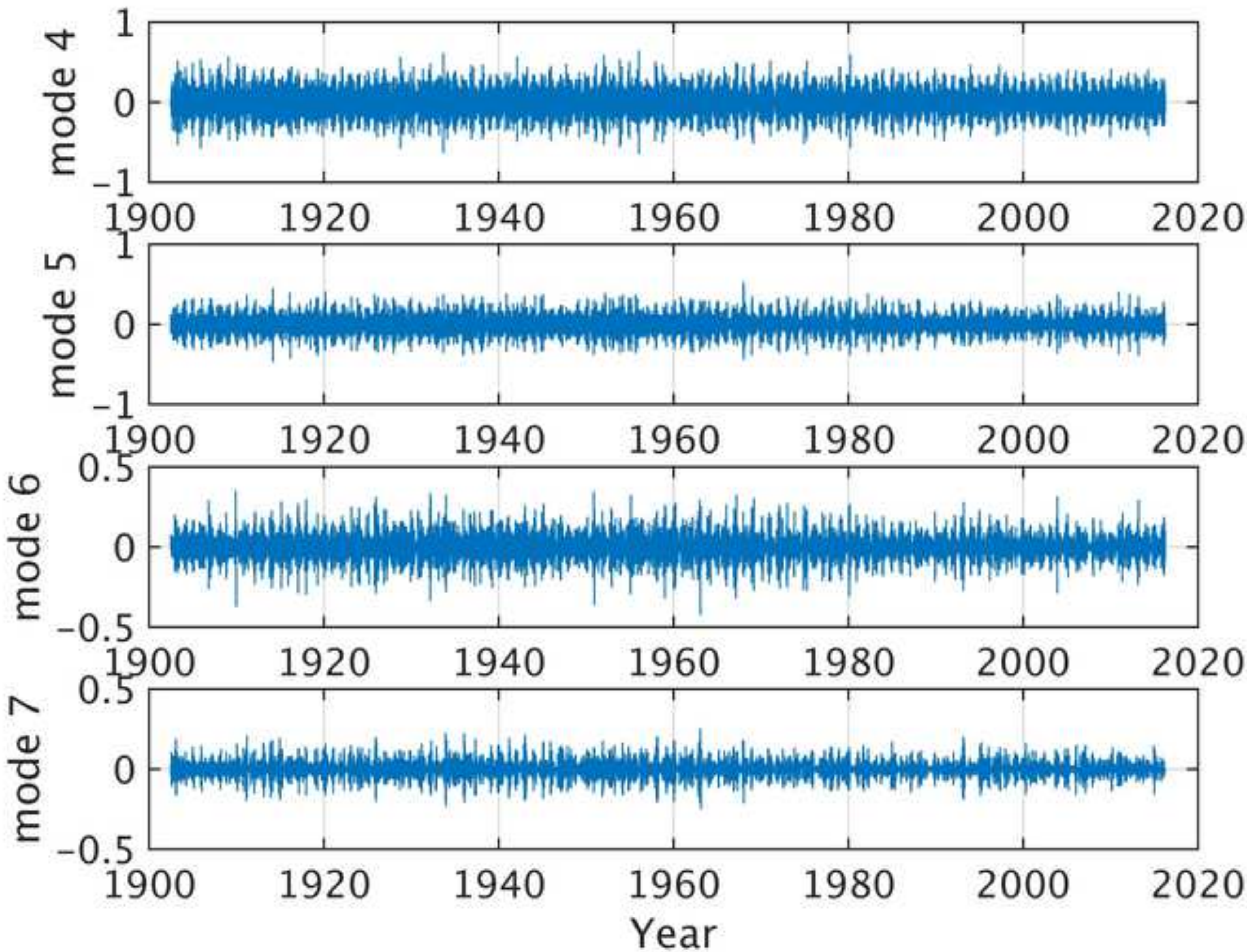

figa_a1c

Click here to download Rendered Figure figa_a1c.jpg

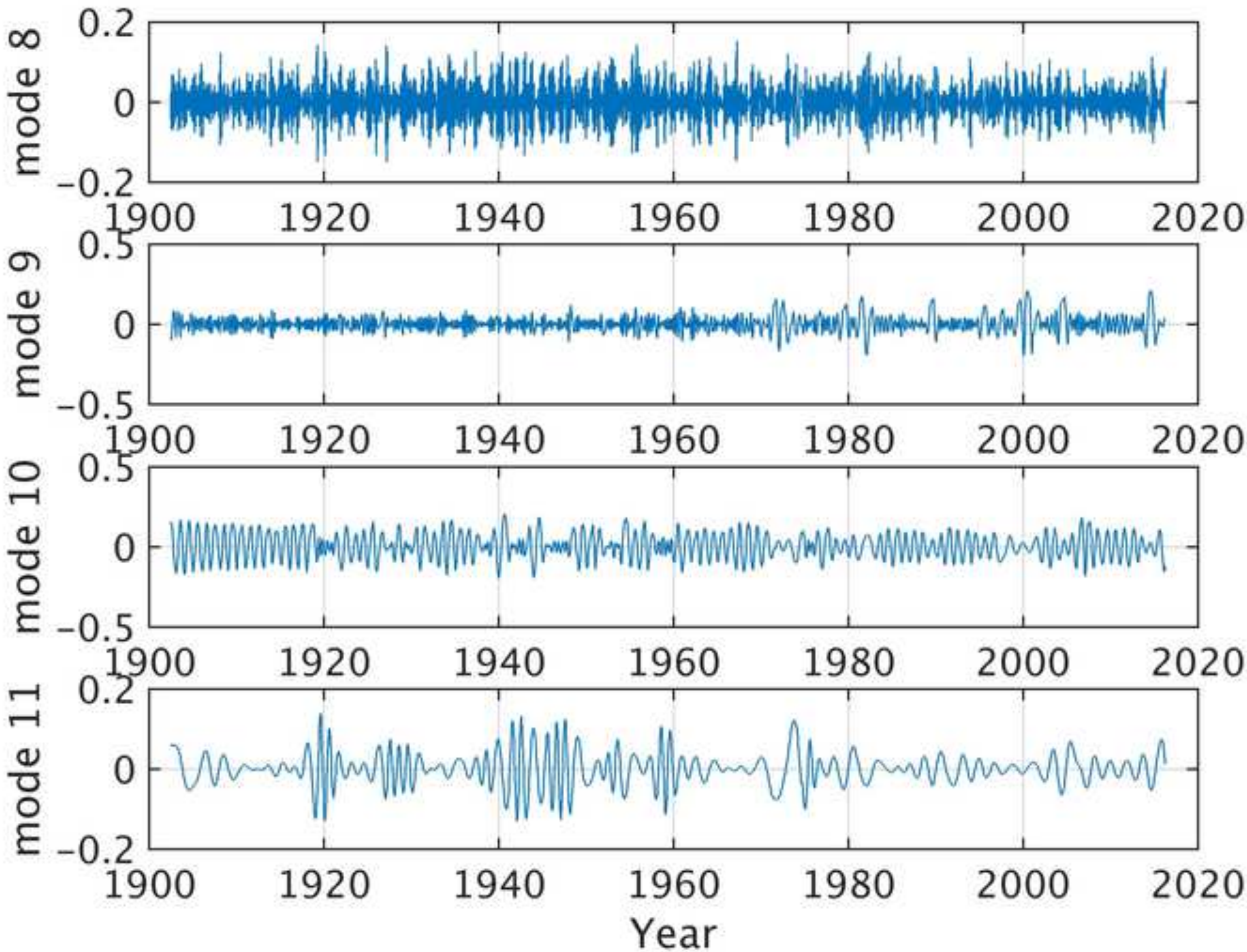

figa_a1d

Click here to download Rendered Figure figa_a1d.jpg

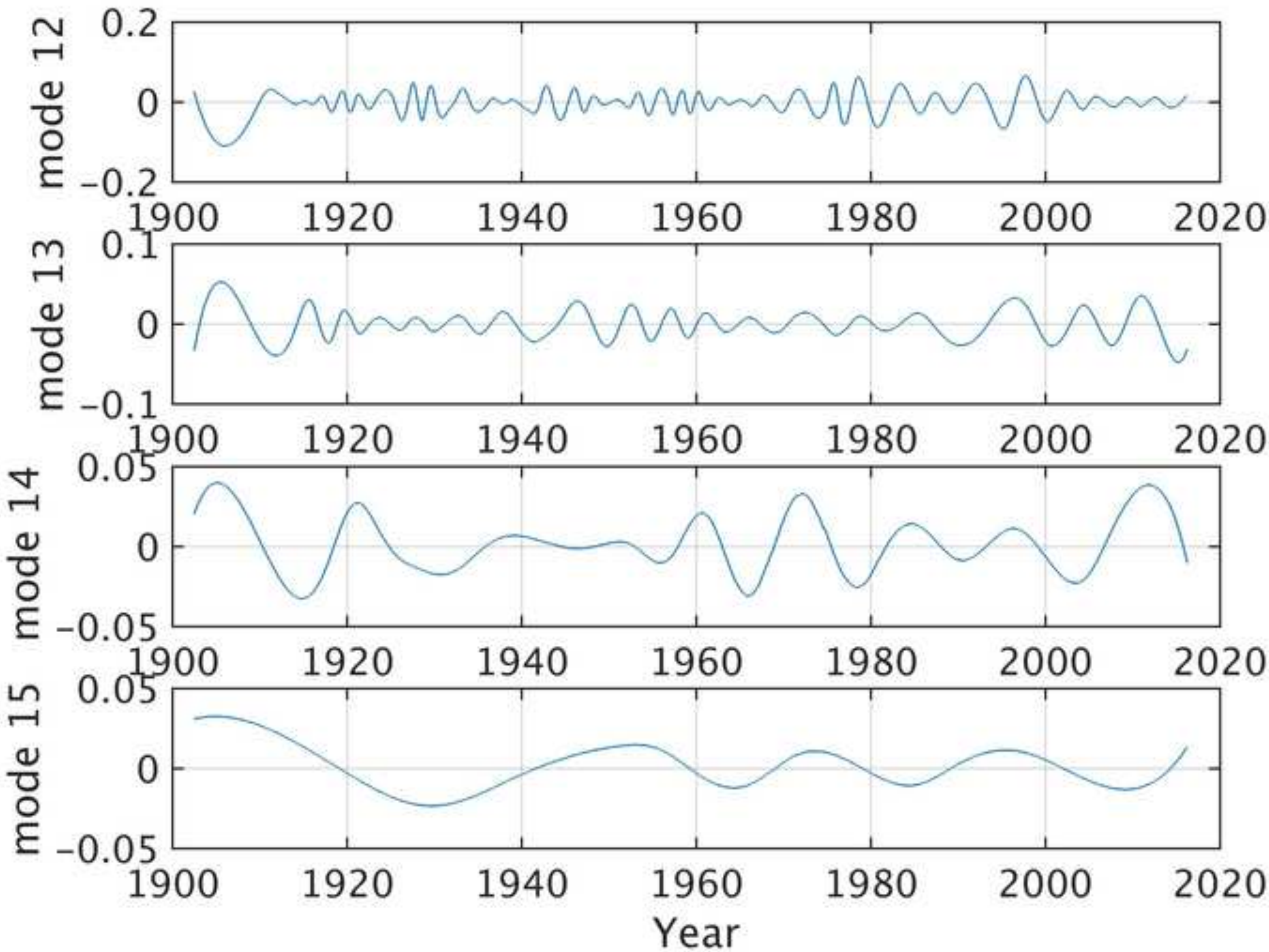

figa_a1e

Click here to download Rendered Figure figa_a1e.jpg

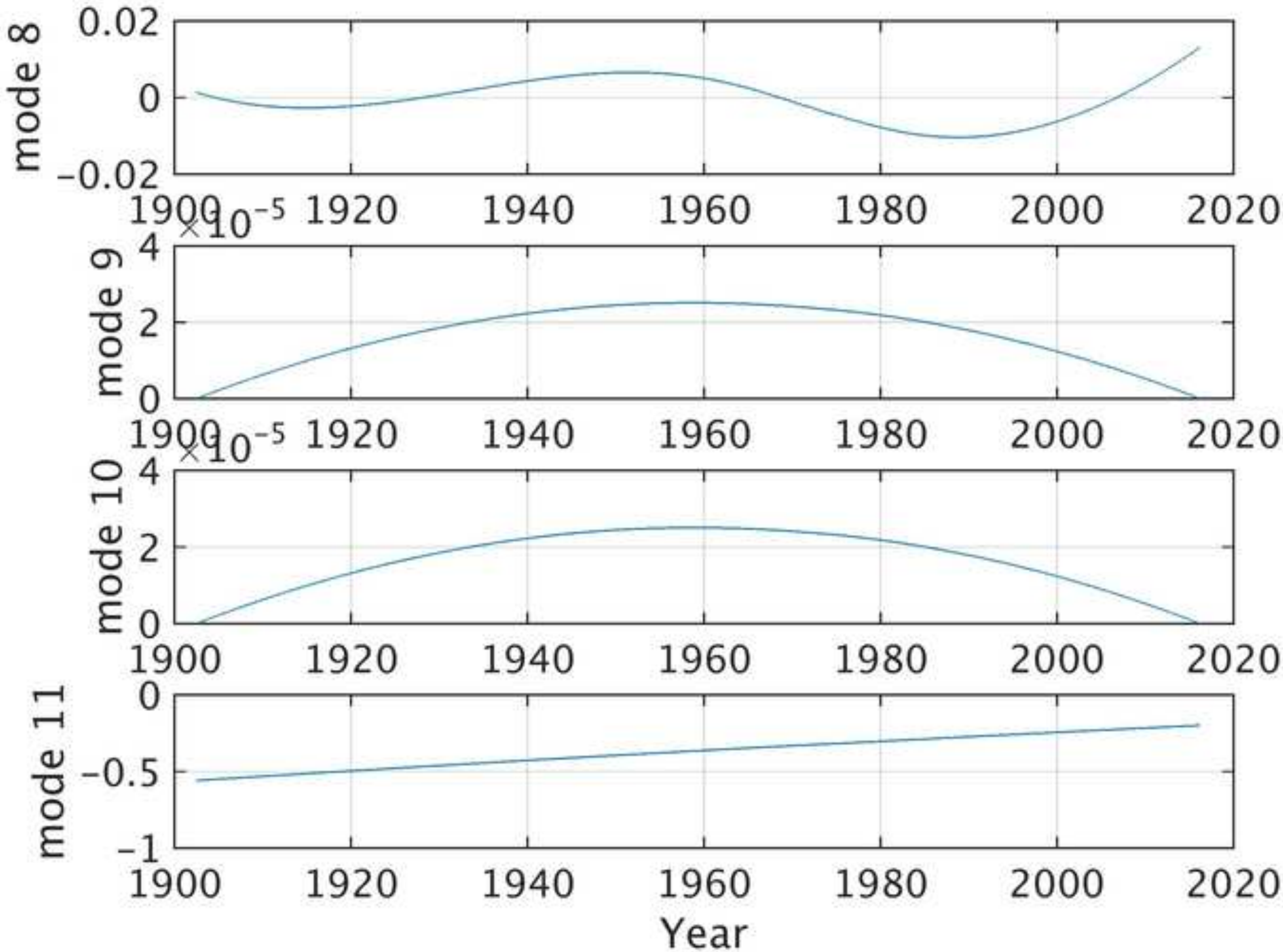

figa2a

Click here to download Rendered Figure figa2a.jpg

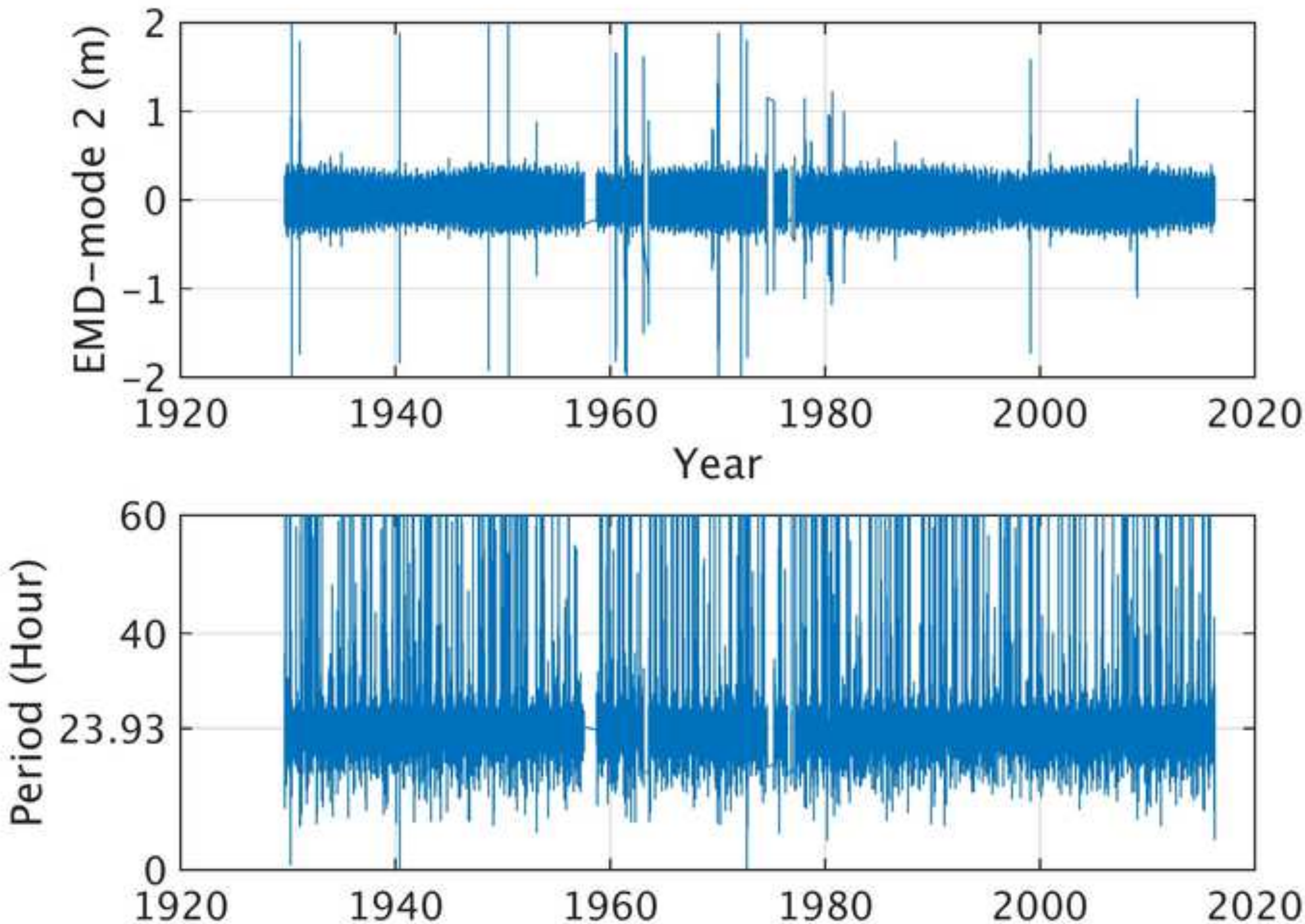

figa2b

Click here to download Rendered Figure figa2b.jpg